9 The strong coupling $\alpha_{\rm s}$

9.1 Introduction

The strong coupling $\bar{g}(\mu)$ defined at scale μ, plays a key role in the understanding of QCD and in its application for collider physics. For example, the parametric uncertainty from α_s is one of the dominant sources of uncertainty in the Standard Model prediction for the $H \to b\bar{b}$ partial width, and the largest source of uncertainty for $H \to gg$. Thus higher precision determinations of α_s are needed to maximize the potential of experimental measurements at the LHC, and for high-precision Higgs studies at future colliders [1–3]. The value of α_s also yields one of the essential boundary conditions for completions of the standard model at high energies.

In order to determine the running coupling at scale μ

$$\alpha_s(\mu) = \frac{\bar{g}^2(\mu)}{4\pi}\,, \tag{230}$$

we should first "measure" a short-distance quantity $\mathcal{Q}$ at scale μ either experimentally or by lattice calculations and then match it with a perturbative expansion in terms of a running coupling, conventionally taken as $\alpha_{\overline{\rm MS}}(\mu)$,

$$\mathcal{Q}(\mu) = c_1\alpha_{\overline{\rm MS}}(\mu) + c_2\alpha_{\overline{\rm MS}}(\mu)^2 + \cdots\,. \tag{231}$$

The essential difference between continuum determinations of α_s and lattice determinations is the origin of the values of $\mathcal{Q}$ in Eq. (231).

The basis of continuum determinations are experimentally measurable cross sections from which $\mathcal{Q}$ is defined. These cross sections have to be sufficiently inclusive and at sufficiently high scales such that perturbation theory can be applied. Often hadronization corrections have to be used to connect the observed hadronic cross sections to the perturbative ones. Experimental data at high μ, where perturbation theory is progressively more precise, usually have increasing experimental errors, and it is not easy to find processes which allow one to follow the μ dependence of a single $\mathcal{Q}(\mu)$ over a range where $\alpha_s(\mu)$ changes significantly and precision is maintained.

In contrast, in lattice gauge theory, one can design $\mathcal{Q}(\mu)$ as Euclidean short-distance quantities which are not directly related to experimental observables. This allows us to follow the μ dependence until the perturbative regime is reached and nonperturbative "corrections" are negligible. The only experimental input for lattice computations of α_s is the hadron spectrum which fixes the overall energy scale of the theory and the quark masses. Therefore experimental errors are completely negligible and issues such as hadronization do not occur. We can construct many short-distance quantities that are easy to calculate nonperturbatively in lattice simulations with small statistical uncertainties. We can also simulate at parameter values that do not exist in nature (for example with unphysical quark masses between bottom and charm) to help control systematic uncertainties. These features mean that precise results for α_s can be achieved with lattice gauge theory computations. Further, as in the continuum, the different methods available to determine α_s in lattice calculations with different associated systematic uncertainties enable valuable cross-checks. Practical limitations are discussed in the next section, but a simple one is worth mentioning here. Experimental results (and therefore the continuum determinations) of course have all quarks present, while in lattice

gauge theories only the light ones are included and one then is forced to use the matching at thresholds, as discussed in the following subsection.

It is important to keep in mind that the dominant source of uncertainty in most present day lattice-QCD calculations of α_s are from the truncation of continuum/lattice perturbation theory and from discretization errors. Perturbative truncation errors are of a different nature than most other lattice (or continuum) systematics, in that they often cannot easily be estimated from studying the data itself. Further, the size of higher-order coefficients in the perturbative series can sometimes turn out to be larger than naive expectations based on power counting from the behaviour of lower-order terms.

The various phenomenological approaches to determining the running coupling, $\alpha^{(5)}_{\overline{\rm MS}}(M_Z)$ are summarized by the Particle Data Group [4]. The PDG review lists 4 categories of phenomenological results used to obtain the running coupling using hadronic τ decays, hadronic final states of e^+e^- annihilation, deep inelastic lepton–nucleon scattering and electroweak precision data. Excluding lattice results, the PDG quotes a weighted average of

$$\alpha^{(5)}_{\overline{\rm MS}}(M_Z) = 0.1175(17)\,, \tag{232}$$

compared to $\alpha^{(5)}_{\overline{\rm MS}}(M_Z) = 0.1183(12)$ of the previous review [5]. For a general overview of the various phenomenological and lattice approaches see e.g. Ref. [6]. We note that perturbative truncation errors are also the dominant source of uncertainty in several of the phenomenological determinations of α_s. In particular, the extraction of α_s from τ data, which is the most precise and has the largest impact on the nonlattice average in Eq. (232) is especially sensitive to the treatment of higher-order perturbative terms. This is important to keep in mind when comparing our chosen range for $\alpha^{(5)}_{\overline{\rm MS}}(M_Z)$ from lattice determinations in Eq. (276) with the nonlattice average from the PDG.

9.1.1 Scheme and scale dependence of α_s and $\Lambda_{\rm QCD}$

Despite the fact that the notion of the QCD coupling is initially a perturbative concept, the associated Λ parameter is nonperturbatively defined

$$\Lambda \equiv \mu\,(b_0\bar{g}^2(\mu))^{-b_1/(2b_0^2)} e^{-1/(2b_0\bar{g}^2(\mu))} \exp\left[-\int_0^{\bar{g}(\mu)} dx \left(\frac{1}{\beta(x)} + \frac{1}{b_0 x^3} - \frac{b_1}{b_0^2 x}\right)\right]\,, \tag{233}$$

where β is the full renormalization group function in the scheme which defines $\bar{g}$, and b_0 and b_1 are the first two scheme-independent coefficients of the perturbative expansion

$$\beta(x) \sim -b_0 x^3 - b_1 x^5 + \ldots\,, \tag{234}$$

with

$$b_0 = \frac{1}{(4\pi)^2}\left(11 - \frac{2}{3}N_f\right)\,, \qquad b_1 = \frac{1}{(4\pi)^4}\left(102 - \frac{38}{3}N_f\right)\,. \tag{235}$$

Thus the Λ parameter is renormalization-scheme-dependent but in an exactly computable way, and lattice gauge theory is an ideal method to relate it to the low-energy properties of QCD.

The change in the coupling from one scheme, S, to another (taken here to be the $\overline{\rm MS}$ scheme) is perturbative,

$$g^2_{\overline{\rm MS}}(\mu) = g^2_{\rm S}(\mu)(1 + c_g^{(1)} g^2_{\rm S}(\mu) + \ldots)\,, \tag{236}$$

where $c_g^{(i)}$ are the finite renormalization coefficients. The scale μ must be taken high enough for the error in keeping only the first few terms in the expansion to be small. On the other hand, the conversion to the Λ parameter in the $\overline{\rm MS}$ scheme is given exactly by

$$\Lambda_{\overline{\rm MS}} = \Lambda_{\rm S} \exp\left[c_g^{(1)}/(2b_0)\right]\,. \tag{237}$$

By convention $\alpha_{\overline{\rm MS}}$ is usually quoted at a scale $\mu = M_Z$ where the appropriate effective coupling is the one in the 5-flavour theory: $\alpha^{(5)}_{\overline{\rm MS}}(M_Z)$. In order to obtain it from a result with fewer flavours, one connects effective theories with different number of flavours as discussed by Bernreuther and Wetzel [7]. For example one considers the $\overline{\rm MS}$ scheme, matches the 3-flavour theory to the 4-flavour theory at a scale given by the charm-quark mass, runs with the 4-loop β-function of the 4-flavour theory to a scale given by the b-quark mass and there matches to the 5-flavour theory, after which one runs up to $\mu = M_Z$. For the matching relation at a given quark threshold we use the mass $m_\star$ which satisfies $m_\star = \overline{m}_{\overline{\rm MS}}(m_\star)$, where $\overline{m}$ is the running mass (analogous to the running coupling). Then

$$\bar{g}^2_{N_f-1}(m_\star) = \bar{g}^2_{N_f}(m_\star) \times [1 + t_2\, \bar{g}^4_{N_f}(m_\star) + t_3\, \bar{g}^6_{N_f}(m_\star) + \ldots] \tag{238}$$

with [8]

$$t_2 = \frac{1}{(4\pi^2)^2}\frac{11}{72} \tag{239}$$

$$t_3 = \frac{1}{(4\pi^2)^3}\left[-\frac{82043}{27648}\zeta_3 + \frac{564731}{124416} - \frac{2633}{31104}(N_f - 1)\right] \tag{240}$$

(where ζ_3 is the Riemann zeta-function) provides the matching at the thresholds in the $\overline{\rm MS}$ scheme. While t_2, t_3 are numerically small coefficients, the charm threshold scale is also relatively low and so there are nonperturbative uncertainties in the matching procedure, which are difficult to estimate but which we assume here to be negligible. Obviously there is no perturbative matching formula across the strange "threshold"; here matching is entirely nonperturbative. Model dependent extrapolations of $\bar{g}^2_{N_f}$ from $N_f = 0, 2$ to $N_f = 3$ were done in the early days of lattice gauge theory. We will include these in our listings of results but not in our estimates, since such extrapolations are based on untestable assumptions.

9.1.2 Overview of the review of α_s

We begin by explaining lattice-specific difficulties in Sec. 9.2 and the FLAG criteria designed to assess whether the associated systematic uncertainties can be controlled and estimated in a reasonable manner. We then discuss, in Sec. 9.3 – Sec. 9.8, the various lattice approaches. For completeness, we present results from calculations with $N_f = 0, 2, 3$, and 4 flavours. Finally, in Sec. 9.9, we present averages together with our best estimates for $\alpha^{(5)}_{\overline{\rm MS}}$. These are determined from 3- and 4-flavour QCD simulations. The earlier $N_f = 0, 2$ works obtained results for $N_f = 3$ by extrapolation in N_f. Because this is not a theoretically controlled

procedure, we do not include these results in our averages. For the Λ parameter, we also give results for other number of flavours, including $N_f = 0$. Even though the latter numbers should not be used for phenomenology, they represent valuable nonperturbative information concerning field theories with variable numbers of quarks.

9.1.3 Differences compared to the FLAG 13 report

For the benefit of the readers who are familiar with our previous report, we list here where changes and additions can be found which go beyond slight improvements of the presentation.

Our criteria are unchanged as far as the explicit ratings on renormalization scale, perturbative behaviour and continuum extrapolation are concerned. However, where we discuss the criteria, we emphasize that it is also important whether finite-size effects and topology sampling are under control. In a few cases, this influences our decision on which computations enter our ranges and averages.

New computations which are reviewed here are

Karbstein 14 [9] and Bazavov 14 [10] based on the static-quark potential (Sec. 9.4),

FlowQCD 15 [11] based on a tadpole-improved bare coupling (Sec. 9.6),

HPQCD 14A [12] based on heavy-quark current two-point functions (Sec. 9.7).

They influence the final ranges marginally.

9.2 Discussion of criteria for computations entering the averages

As in the PDG review, we only use calculations of α_s published in peer-reviewed journals, and that use NNLO or higher-order perturbative expansions, to obtain our final range in Sec. 9.9. We also, however, introduce further criteria designed to assess the ability to control important systematics which we describe here. Some of these criteria, e.g. that for the continuum extrapolation, are associated with lattice-specific systematics and have no continuum analogue. Other criteria, e.g. that for the renormalization scale, could in principle be applied to nonlattice determinations. Expecting that lattice calculations will continue to improve significantly in the near future, our goal in reviewing the state of the art here is to be conservative and avoid prematurely choosing an overly small range.

In lattice calculations, we generally take $\mathcal{Q}$ to be some combination of physical amplitudes or Euclidean correlation functions which are free from UV and IR divergences and have a well-defined continuum limit. Examples include the force between static quarks and 2-point functions of quark bilinear currents.

In comparison to values of observables $\mathcal{Q}$ determined experimentally, those from lattice calculations require two more steps. The first step concerns setting the scale μ in GeV, where one needs to use some experimentally measurable low-energy scale as input. Ideally one employs a hadron mass. Alternatively convenient intermediate scales such as $\sqrt{t_0}$, w_0, r_0, r_1, [13–16] can be used if their relation to an experimental dimensionful observable is established. The low-energy scale needs to be computed at the same bare parameters where $\mathcal{Q}$ is determined, at least as long as one does not use the step-scaling method (see below). This induces a practical difficulty given present computing resources. In the determination of the low-energy reference scale the volume needs to be large enough to avoid finite-size effects. On the other hand, in order for the perturbative expansion of Eq. (231) to be reliable, one

has to reach sufficiently high values of μ, i.e. short enough distances. To avoid uncontrollable discretization effects the lattice spacing a has to be accordingly small. This means

$$L \gg \text{hadron size} \sim \Lambda_{\rm QCD}^{-1} \quad \text{and} \quad 1/a \gg \mu\,, \tag{241}$$

(where L is the box size) and therefore

$$L/a \ggg \mu/\Lambda_{\rm QCD}\,. \tag{242}$$

The currently available computer power, however, limits L/a, typically to $L/a = 20 - 64$. Unless one accepts compromises in controlling discretization errors or finite-size effects, this means one needs to set the scale μ according to

$$\mu \lll L/a \times \Lambda_{\rm QCD} \quad \sim 5 - 20\,\text{GeV}\,. \tag{243}$$

Therefore, μ can be $1 - 3\,\text{GeV}$ at most. This raises the concern whether the asymptotic perturbative expansion truncated at 1-loop, 2-loop, or 3-loop in Eq. (231) is sufficiently accurate. There is a finite-size scaling method, usually called step-scaling method, which solves this problem by identifying $\mu = 1/L$ in the definition of $\mathcal{Q}(\mu)$, see Sec. 9.3.

For the second step after setting the scale μ in physical units (GeV), one should compute $\mathcal{Q}$ on the lattice, $\mathcal{Q}_{\rm lat}(a,\mu)$ for several lattice spacings and take the continuum limit to obtain the left hand side of Eq. (231) as

$$\mathcal{Q}(\mu) \equiv \lim_{a\to 0} \mathcal{Q}_{\rm lat}(a,\mu) \text{ with } \mu \text{ fixed}\,. \tag{244}$$

This is necessary to remove the discretization error.

Here it is assumed that the quantity $\mathcal{Q}$ has a continuum limit, which is regularization-independent up to discretization errors. The method discussed in Sec. 9.6, which is based on the perturbative expansion of a lattice-regulated, divergent short-distance quantity $W_{\rm lat}(a)$ differs in this respect and must be treated separately.

In summary, a controlled determination of α_s needs to satisfy the following:

1. The determination of α_s is based on a comparison of a short-distance quantity $\mathcal{Q}$ at scale μ with a well–defined continuum limit without UV and IR divergences to a perturbative expansion formula in Eq. (231).

2. The scale μ is large enough so that the perturbative expansion in Eq. (231) is precise to the order at which it is truncated, i.e. it has good *asymptotic* convergence.

3. If $\mathcal{Q}$ is defined by physical quantities in infinite volume, one needs to satisfy Eq. (242).

   Nonuniversal quantities need a separate discussion, see Sec. 9.6.

Conditions 2. and 3. give approximate lower and upper bounds for μ respectively. It is important to see whether there is a window to satisfy 2. and 3. at the same time. If it exists, it remains to examine whether a particular lattice calculation is done inside the window or not.

Obviously, an important issue for the reliability of a calculation is whether the scale μ that can be reached lies in a regime where perturbation theory can be applied with confidence. However, the value of μ does not provide an unambiguous criterion. For instance,

the Schrödinger Functional, or SF-coupling (Sec. 9.3) is conventionally taken at the scale $\mu = 1/L$, but one could also choose $\mu = 2/L$. Instead of μ we therefore define an effective $\alpha_{\rm eff}$. For schemes such as SF (see Sec. 9.3) or qq (see Sec. 9.4) this is directly the coupling of the scheme. For other schemes such as the vacuum polarization we use the perturbative expansion Eq. (231) for the observable $\mathcal{Q}$ to define

$$\alpha_{\rm eff} = \mathcal{Q}/c_1 \,. \tag{245}$$

If there is an α_s-independent term it should first be subtracted. Note that this is nothing but defining an effective, regularization-independent coupling, a physical renormalization scheme.

Let us now comment further on the use of the perturbative series. Since it is only an asymptotic expansion, the remainder $R_n(\mathcal{Q}) = \mathcal{Q} - \sum_{i\le n} c_i\alpha_s^i$ of a truncated perturbative expression $\mathcal{Q} \sim \sum_{i\le n} c_i\alpha_s^i$ cannot just be estimated as a perturbative error $k\,\alpha_s^{n+1}$. The error is nonperturbative. Often one speaks of "nonperturbative contributions", but nonperturbative and perturbative cannot be strictly separated due to the asymptotic nature of the series (see e.g. Ref. [17]).

Still, we do have some general ideas concerning the size of nonperturbative effects. The known ones such as instantons or renormalons decay for large μ like inverse powers of μ and are thus roughly of the form

$$\exp(-\gamma/\alpha_s)\,, \tag{246}$$

with some positive constant γ. Thus we have, loosely speaking,

$$\mathcal{Q} = c_1\alpha_s + c_2\alpha_s^2 + \ldots + c_n\alpha_s^n + \mathcal{O}(\alpha_s^{n+1}) + \mathcal{O}(\exp(-\gamma/\alpha_s))\,. \tag{247}$$

For small α_s, the $\exp(-\gamma/\alpha_s)$ is negligible. Similarly the perturbative estimate for the magnitude of relative errors in Eq. (247) is small; as an illustration for $n = 3$ and $\alpha_s = 0.2$ the relative error is $\sim 0.8\%$ (assuming coefficients $|c_{n+1}/c_1| \sim 1$).

For larger values of α_s nonperturbative effects can become significant in Eq. (247). An instructive example comes from the values obtained from τ decays, for which $\alpha_s \approx 0.3$. Here, different applications of perturbation theory (fixed order, FOPT, and contour improved, CIPT) each look reasonably asymptotically convergent but the difference does not seem to decrease much with the order (see, e.g., the contribution of Pich in Ref. [6]). In addition nonperturbative terms in the spectral function may be nonnegligible even after the integration up to m_τ (see, e.g., Ref. [18], Golterman in Ref. [6]). All of this is because α_s is not really small.

Since the size of the nonperturbative effects is very hard to estimate one should try to avoid such regions of the coupling. In a fully controlled computation one would like to verify the perturbative behaviour by changing α_s over a significant range instead of estimating the errors as $\sim \alpha_s^{n+1}$. Some computations try to take nonperturbative power 'corrections' to the perturbative series into account by including such terms in a fit to the μ dependence. We note that this is a delicate procedure, both because the separation of nonperturbative and perturbative is theoretically not well defined and because in practice a term like, e.g., $\alpha_s(\mu)^3$ is hard to distinguish from a $1/\mu^2$ term when the μ-range is restricted and statistical and systematic errors are present. We consider it safer to restrict the fit range to the region where the power corrections are negligible compared to the estimated perturbative error.

The above considerations lead us to the following special criteria for the determination of α_s.

- Renormalization scale

  ★ all points relevant in the analysis have $\alpha_{\rm eff} < 0.2$

  ○ all points have $\alpha_{\rm eff} < 0.4$ and at least one $\alpha_{\rm eff} \leq 0.25$

  ■ otherwise

- Perturbative behaviour

  ★ verified over a range of a factor 4 change in $\alpha_{\rm eff}^{n_{\rm l}}$ without power corrections or alternatively $\alpha_{\rm eff}^{n_{\rm l}} = 0.01$ is reached

  ○ agreement with perturbation theory over a range of a factor 2.25 in $\alpha_{\rm eff}^{n_{\rm l}}$ possibly fitting with power corrections or alternatively $\alpha_{\rm eff}^{n_{\rm l}} = 0.02$ is reached

  ■ otherwise

  Here $n_{\rm l}$ is the loop order to which the connection of $\alpha_{\rm eff}$ to the $\overline{\rm MS}$ scheme is known. The β-function of $\alpha_{\rm eff}$ is then known to $n_{\rm l}+1$ loop order.[1]

- Continuum extrapolation

  At a reference point of $\alpha_{\rm eff} = 0.3$ (or less) we require

  ★ three lattice spacings with $\mu a < 1/2$ and full $\mathcal{O}(a)$ improvement,
  or three lattice spacings with $\mu a \leq 1/4$ and 2-loop $\mathcal{O}(a)$ improvement,
  or $\mu a \leq 1/8$ and 1-loop $\mathcal{O}(a)$ improvement

  ○ three lattice spacings with $\mu a < 1.5$ reaching down to $\mu a = 1$ and full $\mathcal{O}(a)$ improvement,
  or three lattice spacings with $\mu a \leq 1/4$ and 1-loop $\mathcal{O}(a)$ improvement

  ■ otherwise

- Finite-size effects

  These are a less serious issue for the determination of α_s since one looks at short-distance observables where such effects are expected to be suppressed. We therefore have no special criterion in our tables, but do check that volumes are not too small and in particular the scale is determined in large enough volume.[2] Remarks are added in the text when appropriate.

- Topology sampling

  In principle a good way to improve the quality of determinations of α_s is to push to very small lattice spacings thus enabling large μ. It is known that the sampling

[1] Once one is in the perturbative region with $\alpha_{\rm eff}$, the error in extracting the Λ parameter due to the truncation of perturbation theory scales like $\alpha_{\rm eff}^{n_{\rm l}}$, as seen e.g. in Eq. (233). In order to well detect/control such corrections, one needs to change the correction term significantly; we require a factor of four for a ★ and a factor 2.25 for a ○. In comparison to FLAG 13, where $n_l = 2$ was taken as the default, we have made the n_l dependence explicit and list it in Tabs. ?? – ??. An exception to the above is the situation where the correction terms are small anyway, i.e. $\alpha_{\rm eff}^{n_{\rm l}} \approx 0.02$ is reached.

[2] Note also that the determination of the scale does not need to be very precise, since using the lowest-order β-function shows that a 3% error in the scale determination corresponds to a $\sim 0.5\%$ error in $\alpha_s(M_Z)$. So as long as systematic errors from chiral extrapolation and finite-volume effects are below 3% we do not need to be concerned about those. This covers most cases.

of field space becomes very difficult for the HMC algorithm when the lattice spacing is small and one has the standard periodic boundary conditions. In practice, for all known discretizations the topological charge slows down dramatically for $a \approx 0.05\,\text{fm}$ and smaller [19–25]. Open boundary conditions solve the problem [26] but are rarely used. Since the effect of the freezing is generally not known, we also do need to pay attention to this issue. Remarks are added in the text when appropriate.

We assume that quark-mass effects of light quarks (including strange) are negligible in the effective coupling itself where large, perturbative, μ is considered.

We also need to specify what is meant by μ. Here are our choices:

$$\begin{aligned} \text{Schrödinger Functional} &: \mu = 1/L\,, \\ \text{heavy quark-antiquark potential} &: \mu = 2/r\,, \\ \text{observables in momentum space} &: \mu = q\,, \\ \text{moments of heavy-quark currents} &: \mu = 2\bar{m}_{\rm h} \end{aligned} \tag{248}$$

where q is the magnitude of the momentum and $\bar{m}_{\rm h}$ the heavy-quark mass. We note again that the above criteria cannot be applied when regularization dependent quantities $W_{\rm lat}(a)$ are used instead of $\mathcal{O}(\mu)$. These cases are specifically discussed in Sec. 9.6.

A popular scale choice is the intermediate r_0 scale, although one should also bear in mind that its determination from physical observables has also to be taken into account. The phenomenological value of r_0 was originally determined as $r_0 \approx 0.49\,\text{fm}$ through potential models describing quarkonia [15]. Recent determinations from 2-flavour QCD are $r_0 = 0.420(14) - 0.450(14)\,\text{fm}$ by the ETM collaboration [27, 28], using as input f_π and f_K and carrying out various continuum extrapolations. On the other hand, the ALPHA collaboration [29] determined $r_0 = 0.503(10)\,\text{fm}$ with input from f_K, and the QCDSF Collaboration [30] cites $0.501(10)(11)\,\text{fm}$ from the mass of the nucleon (no continuum limit). Recent determinations from 3-flavour QCD are consistent with $r_1 = 0.313(3)\,\text{fm}$ and $r_0 = 0.472(5)\,\text{fm}$ [31–33]. Due to the uncertainty in these estimates, and as many results are based directly on r_0 to set the scale, we shall often give both the dimensionless number $r_0\Lambda_{\overline{\rm MS}}$, as well as $\Lambda_{\overline{\rm MS}}$. In the cases where no physical r_0 scale is given in the original papers or we convert to the r_0 scale, we use the value $r_0 = 0.472\,\text{fm}$. In case $r_1\Lambda_{\overline{\rm MS}}$ is given in the publications, we use $r_0/r_1 = 1.508$ [33] to convert, neglecting the error on this ratio. In some, mostly early, computations the string tension, $\sqrt{\sigma}$ was used. We convert to r_0 using $r_0^2\sigma = 1.65 - \pi/12$, which has been shown to be an excellent approximation in the relevant pure gauge theory [34, 35]. The new scales t_0, w_0 based on the Wilson flow are very attractive alternatives to r_0 but have not yet been used as much and their discretization errors are still under discussion [36–39]. We remain with r_0 as our main reference scale for now.

The attentive reader will have noticed that bounds such as $\mu a < 1.5$ or at least one value of $\alpha_{\rm eff} \leq 0.25$ which we require for a ○ are not very stringent. There is a considerable difference between ○ and ★. We have chosen the above bounds, unchanged as compared to FLAG 13, since not too many computations would satisfy more stringent ones at present. Nevertheless, we believe that the ○ criteria already give reasonable bases for estimates of systematic errors. In the future, we expect that we will be able to tighten our criteria for inclusion in the average, and that many more computations will reach the present ★ rating in one or more categories.

In principle one should also account for electro-weak radiative corrections. However, both in the determination of $\alpha_{\rm s}$ at intermediate scales μ and in the running to high scales, we

expect electro-weak effects to be much smaller than the presently reached precision. Such effects are therefore not further discussed.

9.3 α_s from the Schrödinger Functional

9.3.1 General considerations

The method of step-scaling functions avoids the scale problem, Eq. (241). It is in principle independent of the particular boundary conditions used and was first developed with periodic boundary conditions in a two-dimensional model [40]. However, at present most applications in QCD use Schrödinger functional boundary conditions [41, 42]. An important reason is that these boundary conditions avoid zero modes for the quark fields and quartic modes [43] in the perturbative expansion in the gauge fields. Furthermore the corresponding renormalization scheme is well studied in perturbation theory [44–46] with the 3-loop β-function and 2-loop cutoff effects (for the standard Wilson regularization) known.

Let us first briefly review the step-scaling strategy. The essential idea is to split the determination of the running coupling at large μ and of a hadronic scale into two lattice calculations and connect them by 'step scaling'. In the former part, we determine the running coupling constant in a finite-volume scheme, in practice a 'Schrödinger Functional (SF) scheme' in which the renormalization scale is set by the inverse lattice size $\mu = 1/L$. In this calculation, one takes a high renormalization scale while keeping the lattice spacing sufficiently small as

$$\mu \equiv 1/L \sim 10 \ldots 100\,\mathrm{GeV}\,, \qquad a/L \ll 1\,. \tag{249}$$

In the latter part, one chooses a certain $\bar{g}^2_{\mathrm{max}} = \bar{g}^2(1/L_{\mathrm{max}})$, typically such that L_{max} is around 0.5 fm. With a common discretization, one then determines L_{max}/a and (in a large volume $L \geq 2-3\,\mathrm{fm}$) a hadronic scale such as a hadron mass, $\sqrt{t_0}/a$ or r_0/a at the same bare parameters. In this way one gets numbers for L_{max}/r_0 and by changing the lattice spacing a carries out a continuum limit extrapolation of that ratio.

In order to connect $\bar{g}^2(1/L_{\mathrm{max}})$ to $\bar{g}^2(\mu)$ at high μ, one determines the change of the coupling in the continuum limit when the scale changes from L to $L/2$, starting from $L = L_{\mathrm{max}}$ and arriving at $\mu = 2^k/L_{\mathrm{max}}$. This part of the strategy is called step scaling. Combining these results yields $\bar{g}^2(\mu)$ at $\mu = 2^k \frac{r_0}{L_{\mathrm{max}}} r_0^{-1}$, where r_0 stands for the particular chosen hadronic scale.

In order to have a perturbatively well-defined scheme, the SF scheme uses Dirichlet boundary condition at time $t = 0$ and $t = T$. These break translation invariance and permit $\mathcal{O}(a)$ counter terms at the boundary through quantum corrections. Therefore, the leading discretization error is $\mathcal{O}(a)$. Improving the lattice action is achieved by adding counter terms at the boundaries whose coefficients are denoted as $c_t, \tilde{c}_t$. In practice, these coefficients are computed with 1-loop or 2-loop perturbative accuracy. A better precision in this step yields a better control over discretization errors, which is important, as can be seen, e.g., in Refs. [34, 47]. The finite $c_g^{(i)}$, Eq. (236), are known for $i = 1, 2$ [45, 46].

Also computations with Dirichlet boundary conditions do in principle suffer from the insufficient change of topology in the HMC algorithm at small lattice spacing. However, in a small volume the weight of nonzero charge sectors in the path integral is exponentially suppressed [48] [3] and one practically should not sample any nontrivial topology. Considering

[3] We simplify here and assume that the classical solution associated with the used boundary conditions has charge zero. In practice this is the case.

the suppression quantitatively Ref. [49] finds a strong suppression below $L \approx 0.8\,\text{fm}$. Therefore the lack of topology change of the HMC is not a real issue in the computations discussed here. A mix of Dirichlet and open boundary conditions is expected to remove this worry [50] and may be considered in the future.

9.3.2 Discussion of computations

In Tab. 44 we give results from various determinations of the Λ parameter. For a clear

Collaboration	Ref.	N_f	publication status	renormalization scale	perturbative behaviour	continuum extrapolation	scale	$\Lambda_{\overline{\text{MS}}}$[MeV]	$r_0\Lambda_{\overline{\text{MS}}}$
ALPHA 10A	[51]	4	A	★	★	★	only running of α_s in Fig. 4		
Perez 10	[52]	4	P	★	★	○	only step-scaling function in Fig. 4		
PACS-CS 09A	[53]	2+1	A	★	★	○	m_ρ	$371(13)(8)(^{+0}_{-27})^{\#}$	$0.888(30)(18)(^{+0}_{-65})^{\dagger}$
			A	★	★	○	m_ρ	$345(59)^{\#\#}$	$0.824(141)^{\dagger}$
ALPHA 12*	[29]	2	A	★	★	★	f_K	310(20)	0.789(52)
ALPHA 04	[54]	2	A	■	★	★	$r_0 = 0.5\,\text{fm}^{\S}$	$245(16)(16)^{\S}$	$0.62(2)(2)^{\S}$
ALPHA 01A	[55]	2	A	★	★	★	only running of α_s in Fig. 5		
CP-PACS 04$^{\&}$	[47]	0	A	★	★	○	only tables of g^2_{SF}		
ALPHA 98††	[56]	0	A	★	★	○	$r_0 = 0.5\text{fm}$	238(19)	0.602(48)
Lüscher 93	[44]	0	A	★	○	○	$r_0 = 0.5\text{fm}$	233(23)	$0.590(60)^{\S\S}$

$^{\#}$ Result with a constant (in a) continuum extrapolation of the combination $L_{\max}m_\rho$.
† In conversion to $r_0\Lambda_{\overline{\text{MS}}}$, r_0 is taken to be 0.472 fm.
$^{\#\#}$ Result with a linear continuum extrapolation in a of the combination $L_{\max}m_\rho$.
* Supersedes ALPHA 04.
§ The $N_f = 2$ results were based on values for r_0/a which have later been found to be too small by [29]. The effect will be of the order of 10–15%, presumably an increase in Λr_0. We have taken this into account by a ■ in the renormalization scale.
$^{\&}$ This investigation was a precursor for PACS-CS 09A and confirmed two step-scaling functions as well as the scale setting of ALPHA 98.
†† Uses data of Lüscher 93 and therefore supersedes it.
§§ Converted from $\alpha_{\overline{\text{MS}}}(37r_0^{-1}) = 0.1108(25)$.

Table 44: Results for the Λ parameter from computations using step scaling of the SF-coupling. Entries without values for Λ computed the running and established perturbative behaviour at large μ.

assessment of the N_f dependence, the last column also shows results that refer to a common hadronic scale, r_0. As discussed above, the renormalization scale can be chosen large enough

such that $\alpha_s < 0.2$ and the perturbative behaviour can be verified. Consequently only ★ is present for these criteria except for early work where the $n_l = 2$ loop connection to $\overline{\rm MS}$ was not yet known. With dynamical fermions, results for the step-scaling functions are always available for at least $a/L = \mu a = 1/4, 1/6, 1/8$. All calculations have a nonperturbatively $\mathcal{O}(a)$ improved action in the bulk. For the discussed boundary $\mathcal{O}(a)$ terms this is not so. In most recent calculations 2-loop $\mathcal{O}(a)$ improvement is employed together with at least three lattice spacings.[4] This means a ★ for the continuum extrapolation. In the other contributions only 1-loop c_t was available and we arrive at ○. We note that the discretization errors in the step-scaling functions are usually found to be very small, at the percent level or below. However, the overall desired precision is very high as well, and the results in CP-PACS 04 [47] show that discretization errors at the below percent level cannot be taken for granted. In particular with staggered fermions (unimproved except for boundary terms) few percent effects are seen in Perez 10 [52].

In the work by PACS-CS 09A [53], the continuum extrapolation in the scale setting is performed using a constant function in a and with a linear function. Potentially the former leaves a considerable residual discretization error. We here use, as discussed with the collaboration, the continuum extrapolation linear in a, as given in the second line of PACS-CS 09A [53] results in Tab. 44.

A single computation, PACS-CS 09A [53], quotes also $\alpha_{\overline{\rm MS}}(M_Z)$. We take the linear continuum extrapolation as discussed above:

$$\alpha^{(5)}_{\overline{\rm MS}}(M_Z) = 0.118(3)\,, \tag{250}$$

where the conversion from a 3-flavour result to 5-flavours was done perturbatively (see Sec. 9.2). Other results do not have a sufficient number of quark flavours (ALPHA 10A [51], Perez 10 [52]) or do not yet contain the conversion of the scale to physical units. Thus no value for $\alpha^{(5)}_{\overline{\rm MS}}(M_Z)$ is quoted.

More results for $\alpha^{(5)}_{\overline{\rm MS}}(M_Z)$ using step-scaling functions can be expected soon. Their precision is likely to be much better than what we were able to report on here. A major reason is the use of the gradient flow [13] in definitions of finite volume schemes [57, 58].

9.4 α_s from the potential at short distances

9.4.1 General considerations

The basic method was introduced in Ref. [59] and developed in Ref. [60]. The force or potential between an infinitely massive quark and antiquark pair defines an effective coupling constant via

$$F(r) = \frac{dV(r)}{dr} = C_F \frac{\alpha_{\rm qq}(r)}{r^2}\,. \tag{251}$$

The coupling can be evaluated nonperturbatively from the potential through a numerical differentiation, see below. In perturbation theory one also defines couplings in different schemes $\alpha_{\bar V}$, α_V via

$$V(r) = -C_F \frac{\alpha_{\bar V}(r)}{r}\,, \qquad \text{or} \quad \tilde V(Q) = -C_F \frac{\alpha_V(Q)}{Q^2}\,, \tag{252}$$

[4] With 2-loop $\mathcal{O}(a)$ improvement we here mean $c_{\rm t}$ including the g_0^4 term and $\tilde c_{\rm t}$ with the g_0^2 term. For gluonic observables such as the running coupling this is sufficient for cutoff effects being suppressed to $\mathcal{O}(g^6 a)$.

where one fixes the unphysical constant in the potential by $\lim_{r\to\infty} V(r) = 0$ and $\tilde{V}(Q)$ is the Fourier transform of $V(r)$. Nonperturbatively, the subtraction of a constant in the potential introduces an additional renormalization constant, the value of $V(r_{\rm ref})$ at some distance $r_{\rm ref}$. Perturbatively, it is believed to entail a renormalon ambiguity. In perturbation theory, these definitions are all simply related to each other, and their perturbative expansions are known including the α_s^4 and $\alpha_s^5 \log \alpha_s$ terms [61–68].

The potential $V(r)$ is determined from ratios of Wilson loops, $W(r,t)$, which behave as

$$\langle W(r,t)\rangle = |c_0|^2 e^{-V(r)t} + \sum_{n\neq 0} |c_n|^2 e^{-V_n(r)t}\,, \tag{253}$$

where t is taken as the temporal extension of the loop, r is the spatial one and V_n are excited-state potentials. To improve the overlap with the ground state, and to suppress the effects of excited states, t is taken large. Also various additional techniques are used, such as a variational basis of operators (spatial paths) to help in projecting out the ground state. Furthermore some lattice-discretization effects can be reduced by averaging over Wilson loops related by rotational symmetry in the continuum.

In order to reduce discretization errors it is of advantage to define the numerical derivative giving the force as

$$F(r_{\rm I}) = \frac{V(r) - V(r-a)}{a}\,, \tag{254}$$

where $r_{\rm I}$ is chosen so that at tree level the force is the continuum force. $F(r_{\rm I})$ is then a 'tree-level improved' quantity and similarly the tree-level improved potential can be defined [69].

Lattice potential results are in position space, while perturbation theory is naturally computed in momentum space at large momentum. Usually, the Fourier transform is then taken of the perturbation expansion to match to the lattice data.

Finally, as was noted in Sec. 9.2, a determination of the force can also be used to determine the r_0 scale, by defining it from the static force by

$$r_0^2 F(r_0) = 1.65\,, \tag{255}$$

and with $r_1^2 F(r_1) = 1$ the r_1 scale.

9.4.2 Discussion of computations

In Tab. 45, we list results of determinations of $r_0\Lambda_{\overline{\rm MS}}$ (together with $\Lambda_{\overline{\rm MS}}$ using the scale determination of the authors). Since the last review, FLAG 13, there have been two new computations, Karbstein 14 [9] and Bazavov 14 [10].

The first determinations in the three-colour Yang Mills theory are by UKQCD 92 [60] and Bali 92 [73] who used $\alpha_{\rm qq}$ as explained above, but not in the tree-level improved form. Rather a phenomenologically determined lattice artifact correction was subtracted from the lattice potentials. The comparison with perturbation theory was on a more qualitative level on the basis of a 2-loop β-function ($n_l = 1$) and a continuum extrapolation could not be performed as yet. A much more precise computation of $\alpha_{\rm qq}$ with continuum extrapolation was performed in Refs. [34, 69]. Satisfactory agreement with perturbation theory was found [69] but the stability of the perturbative prediction was not considered sufficient to be able to extract a Λ parameter.

Collaboration	Ref.	N_f	publication status	renormalization scale	perturbative behaviour	continuum extrapolation	scale	$\Lambda_{\overline{\rm MS}}$[MeV]	$r_0\Lambda_{\overline{\rm MS}}$
Bazavov 14	[10]	2+1	A	○	★	○	$r_1 = 0.3106(17)$ fm[a]	$315(^{+18}_{-12})$[b]	$0.746(^{+42}_{-27})$
Bazavov 12	[70]	2+1	A	○†	○	○#	$r_0 = 0.468$ fm	295(30) ⋆	0.70(7)⋆⋆
Karbstein 14	[9]	2	A	○	○	○	$r_0 = 0.42$ fm	331(21)	0.692(31)
ETM 11C	[71]	2	A	○	○	○	$r_0 = 0.42$ fm	315(30)§	0.658(55)
Brambilla 10	[72]	0	A	○	★	○††		266(13)+	$0.637(^{+32}_{-30})$††
UKQCD 92	[60]	0	A	★	○++	■	$\sqrt{\sigma} = 0.44$ GeV	256(20)	0.686(54)
Bali 92	[73]	0	A	★	○++	■	$\sqrt{\sigma} = 0.44$ GeV	247(10)	0.661(27)

[a] Determination on lattices with $m_\pi L = 2.2 - 2.6$. About 10 changes of topological charge on the finest lattice [24]. Scale from r_1 [24] as determined from f_π in Ref. [32].
[b] $\alpha^{(3)}_{\overline{\rm MS}}(1.5\,{\rm GeV}) = 0.336(^{+12}_{-8})$, $\alpha^{(5)}_{\overline{\rm MS}}(M_Z) = 0.1166(^{+12}_{-8})$.
† Since values of $\alpha_{\rm eff}$ within our designated range are used, we assign a ○ despite values of $\alpha_{\rm eff}$ up to $\alpha_{\rm eff} = 0.5$ being used.
# Since values of $2a/r$ within our designated range are used, we assign a ○ although only values of $2a/r \geq 1.14$ are used at $\alpha_{\rm eff} = 0.3$.
⋆ Using results from Ref. [33].
⋆⋆ $\alpha^{(3)}_{\overline{\rm MS}}(1.5\,{\rm GeV}) = 0.326(19)$, $\alpha^{(5)}_{\overline{\rm MS}}(M_Z) = 0.1156(^{+21}_{-22})$.
§ Both potential and r_0/a are determined on a small ($L = 3.2r_0$) lattice.
†† Uses lattice results of Ref. [34], some of which have very small lattice spacings where according to more recent investigations a bias due to the freezing of topology may be present.
+ Only $r_0\Lambda_{\overline{\rm MS}}$ is given, our conversion using $r_0 = 0.472$ fm.
++ We give a ○ because only a NLO formula is used and the error bars are very large; our criterion does not apply well to these very early calculations.

Table 45: Short-distance potential results.

In Brambilla 10 [72] the same quenched lattice results of Ref. [69] were used and a fit was performed to the continuum potential, instead of the force. Perturbation theory to $n_l = 3$ loop was used including a resummation of terms $\alpha_s^3(\alpha_s \ln \alpha_s)^n$ and $\alpha_s^4(\alpha_s \ln \alpha_s)^n$. Close agreement with perturbation theory was found when a renormalon subtraction was performed. Note that the renormalon subtraction introduces a second scale into the perturbative formula which is absent when the force is considered.

Bazavov 14 [10] is an update of Bazavov 12 [70] and modify this procedure somewhat. They consider the well-defined perturbative expansion for the force, where renormalon problems disappear. They set $\mu = 1/r$ to eliminate logarithms and then integrate the force to obtain an expression for the potential. The resulting integration constant is fixed by requiring the perturbative potential to be equal to the nonperturbative one exactly at a reference distance $r_{\rm ref}$ and the two are then compared at other values of r. As a further check, the force is also used directly.

For the quenched calculation Brambilla 10 [72] very small lattice spacings were available, $a \sim 0.025\,\text{fm}$, [69]. For ETM 11C [71], Bazavov 12 [70], Karbstein 14 [9] and Bazavov 14 [10] using dynamical fermions such small lattice spacings are not yet realized (Bazavov 14 reaches down to $a \sim 0.041\,\text{fm}$). They all use the tree-level improved potential as described above. We note that the value of $\Lambda_{\overline{\text{MS}}}$ in physical units by ETM 11C [71] is based on a value of $r_0 = 0.42$ fm. This is at least 10% smaller than the large majority of other values of r_0. Also the value of r_0/a or r_1/a on the finest lattices in ETM 11C [71] and Bazavov 14 [10] come from rather small lattices with $m_\pi L \approx 2.4$, 2.2 respectively.

Instead of the procedure discussed previously, Karbstein 14 [9] reanalyzes the data of ETM 11C [71] by first estimating the Fourier transform $\tilde{V}(p)$ of $V(r)$ and then fits the perturbative expansion of $\tilde{V}(p)$ in terms of $\alpha_{\overline{\text{MS}}}(p)$. Of course, the Fourier transform cannot be computed without modelling the r-dependence of $V(r)$ at short and at large distances. The authors fit a linearly rising potential at large distances together with string-like corrections of order r^{-n} and define the potential at large distances by this fit.[5] Recall that for observables in momentum space we take the renormalization scale entering our criteria as $\mu = p$, Eq. (248). The analysis (as in ETM 11C [71]) is dominated by the data at the smallest lattice spacing, where a controlled determination of the overall scale is difficult due to possible finite-size effects.

One of the main issues for all these computations is whether the perturbative running of the coupling constant has been reached. While for quenched or $N_f = 0$ fermions this seems to be the case at the smallest distances, for dynamical fermions at present there is no consensus. Brambilla 10 [72], Bazavov 12 [70] and Bazavov 14 [10] report good agreement with perturbation theory after the renormalon is subtracted or eliminated, but Ref. [74] uses the force directly, where no renormalon contributes, and finds that far shorter distances are needed than are presently accessible for dynamical fermion simulations in order to match to perturbation theory. Further work is needed to clarify this point.

A second issue is the coverage of configuration space in some of the simulations, which use very small lattice spacings with periodic boundary conditions. Affected are the smallest two lattice spacings of Bazavov 14 [10] where very few tunnelings of the topological charge occur [24]. With present knowledge, it also seems possible that the older data by Refs. [34, 69] used by Brambilla 10 [72] are partially done in (close to) frozen topology.

9.5 α_s from the vacuum polarization at short distances

9.5.1 General considerations

The vacuum polarization function for the flavour nonsinglet currents J^a_μ $(a = 1, 2, 3)$ in the momentum representation is parameterized as

$$\langle J^a_\mu J^b_\nu \rangle = \delta^{ab}[(\delta_{\mu\nu}Q^2 - Q_\mu Q_\nu)\Pi^{(1)}(Q) - Q_\mu Q_\nu \Pi^{(0)}(Q)]\,, \tag{256}$$

where Q_μ is a space like momentum and $J_\mu \equiv V_\mu$ for a vector current and $J_\mu \equiv A_\mu$ for an axial-vector current. Defining $\Pi_J(Q) \equiv \Pi^{(0)}_J(Q) + \Pi^{(1)}_J(Q)$, the operator product expansion

[5] Note that at large distances, where string breaking is known to occur, this is not any more the ground state potential defined by Eq. (253).

(OPE) of the vacuum polarization function $\Pi_{V+A}(Q) = \Pi_V(Q) + \Pi_A(Q)$ is given by

$$\begin{aligned}\Pi_{V+A}|_{\rm OPE}(Q^2,\alpha_s) \\ = \; & c + C_1(Q^2) + C_m^{V+A}(Q^2)\frac{\bar{m}^2(Q)}{Q^2} + \sum_{q=u,d,s} C_{\bar{q}q}^{V+A}(Q^2)\frac{\langle m_q\bar{q}q\rangle}{Q^4} \\ & + C_{GG}(Q^2)\frac{\langle\alpha_s GG\rangle}{Q^4} + \mathcal{O}(Q^{-6})\,,\end{aligned} \tag{257}$$

for large Q^2. $C_X^{V+A}(Q^2) = \sum_{i\geq 0}\left(C_X^{V+A}\right)^{(i)}\alpha_s^i(Q^2)$ are the perturbative coefficient functions for the operators X ($X = 1$, $\bar{q}q$, GG) and $\bar{m}$ is the running mass of the mass-degenerate up and down quarks. C_1 is known including α_s^4 in a continuum renormalization scheme such as the $\overline{\rm MS}$ scheme [75–77]. Nonperturbatively, there are terms in C_X which do not have a series expansion in α_s. For an example for the unit operator see Ref. [78]. The term c is Q–independent and divergent in the limit of infinite ultraviolet cutoff. However the Adler function defined as

$$D(Q^2) \equiv -Q^2\frac{d\Pi(Q^2)}{dQ^2}\,, \tag{258}$$

is a scheme-independent finite quantity. Therefore one can determine the running coupling constant in the $\overline{\rm MS}$ scheme from the vacuum polarization function computed by a lattice-QCD simulation. In more detail, the lattice data of the vacuum polarization is fitted with the perturbative formula Eq. (257) with fit parameter $\Lambda_{\overline{\rm MS}}$ parameterizing the running coupling $\alpha_{\overline{\rm MS}}(Q^2)$.

While there is no problem in discussing the OPE at the nonperturbative level, the 'condensates' such as $\langle\alpha_s GG\rangle$ are ambiguous, since they mix with lower-dimensional operators including the unity operator. Therefore one should work in the high-Q^2 regime where power corrections are negligible within the given accuracy. Thus setting the renormalization scale as $\mu \equiv \sqrt{Q^2}$, one should seek, as always, the window $\Lambda_{\rm QCD} \ll \mu \ll a^{-1}$.

9.5.2 Discussion of computations

Results using this method are, to date, only available using overlap fermions. These are collected in Tab. 46 for $N_f = 2$, JLQCD/TWQCD 08C [80] and for $N_f = 2+1$, JLQCD 10 [79]. At present, only one lattice spacing $a \approx 0.11$ fm has been simulated.

The fit to Eq. (257) is done with the 4-loop relation between the running coupling and $\Lambda_{\overline{\rm MS}}$. It is found that without introducing condensate contributions, the momentum scale where the perturbative formula gives good agreement with the lattice results is very narrow, $aQ \simeq 0.8 - 1.0$. When condensate contributions are included the perturbative formula gives good agreement with the lattice results for the extended range $aQ \simeq 0.6 - 1.0$. Since there is only a single lattice spacing there is a ■ for the continuum limit. The renormalization scale μ is in the range of $Q = 1.6 - 2\,$GeV. Approximating $\alpha_{\rm eff} \approx \alpha_{\overline{\rm MS}}(Q)$, we estimate that $\alpha_{\rm eff} = 0.25 - 0.30$ for $N_f = 2$ and $\alpha_{\rm eff} = 0.29 - 0.33$ for $N_f = 2+1$. Thus we give a ○ and ■ for $N_f = 2$ and $N_f = 2+1$ respectively for the renormalization scale and a ■ for the perturbative behaviour.

We note that more investigations of this method are in progress [81].

Collaboration	Ref.	N_f	publication status	renormalization scale	perturbative behaviour	continuum extrapolation	scale	$\Lambda_{\overline{\rm MS}}$[MeV]	$r_0\Lambda_{\overline{\rm MS}}$
JLQCD 10	[79]	2+1	A	■	■	■	$r_0 = 0.472\,\text{fm}$	247(5)†	0.591(12)
JLQCD/TWQCD 08C	[80]	2	A	○	■	■	$r_0 = 0.49\,\text{fm}$	$234(9)(^{+16}_{-0})$	$0.581(22)(^{+40}_{-0})$

† $\alpha^{(5)}_{\overline{\rm MS}}(M_Z) = 0.1118(3)(^{+16}_{-17})$.

Table 46: Vacuum polarization results.

9.6 α_s from observables at the lattice spacing scale

9.6.1 General considerations

The general method is to evaluate a short-distance quantity $\mathcal{Q}$ at the scale of the lattice spacing $\sim 1/a$ and then determine its relationship to $\alpha_{\overline{\rm MS}}$ via a power series expansion.

This is epitomized by the strategy of the HPQCD collaboration [82, 83], discussed here for illustration, which computes and then fits to a variety of short-distance quantities, Y,

$$Y = \sum_{n=1}^{n_{\rm max}} c_n \alpha^n_{\rm V'}(q^*)\,. \tag{259}$$

Y is taken as the logarithm of small Wilson loops (including some nonplanar ones), Creutz ratios, 'tadpole-improved' Wilson loops and the tadpole-improved or 'boosted' bare coupling ($\mathcal{O}(20)$ quantities in total). c_n are perturbative coefficients (each depending on the choice of Y) known to $n = 3$ with additional coefficients up to $n_{\rm max}$ being numerically fitted. $\alpha_{\rm V'}$ is the running coupling constant related to $\alpha_{\rm V}$ from the static-quark potential (see Sec. 9.4).[6]

The coupling constant is fixed at a scale $q^* = d/a$. This is chosen as the mean value of $\ln q$ with the one gluon loop as measure [84, 85]. (Thus a different result for d is found for every short-distance quantity.) A rough estimate yields $d \approx \pi$, and in general the renormalization scale is always found to lie in this region.

For example for the Wilson loop $W_{mn} \equiv \langle W(ma, na)\rangle$ we have

$$\ln\left(\frac{W_{mn}}{u_0^{2(m+n)}}\right) = c_1\alpha_{\rm V'}(q^*) + c_2\alpha^2_{\rm V'}(q^*) + c_3\alpha^3_{\rm V'}(q^*) + \cdots\,, \tag{260}$$

for the tadpole-improved version, where $c_1, c_2, \ldots$ are the appropriate perturbative coefficients and $u_0 = W_{11}^{1/4}$. Substituting the nonperturbative simulation value in the left hand side, we can determine $\alpha_{\rm V'}(q^*)$, at the scale q^*. Note that one finds empirically that perturbation

[6] $\alpha_{\rm V'}$ is defined by $\Lambda_{\rm V'} = \Lambda_{\rm V}$ and $b_i^{\rm V'} = b_i^{\rm V}$ for $i = 0, 1, 2$ but $b_i^{\rm V'} = 0$ for $i \geq 3$.

theory for these tadpole-improved quantities have smaller c_n coefficients and so the series has a faster apparent convergence.

Using the β-function in the V′ scheme, results can be run to a reference value, chosen as $\alpha_0 \equiv \alpha_{V'}(q_0)$, $q_0 = 7.5\,\text{GeV}$. This is then converted perturbatively to the continuum $\overline{\text{MS}}$ scheme

$$\alpha_{\overline{\text{MS}}}(q_0) = \alpha_0 + d_1\alpha_0^2 + d_2\alpha_0^3 + \cdots , \tag{261}$$

where d_1, d_2 are known one and two loop coefficients.

Other collaborations have focused more on the bare 'boosted' coupling constant and directly determined its relationship to $\alpha_{\overline{\text{MS}}}$. Specifically, the boosted coupling is defined by

$$\alpha_{\text{P}}(1/a) = \frac{1}{4\pi}\frac{g_0^2}{u_0^4} , \tag{262}$$

again determined at a scale $\sim 1/a$. As discussed previously since the plaquette expectation value in the boosted coupling contains the tadpole diagram contributions to all orders, which are dominant contributions in perturbation theory, there is an expectation that the perturbation theory using the boosted coupling has smaller perturbative coefficients [84], and hence smaller perturbative errors.

9.6.2 Continuum limit

Lattice results always come along with discretization errors, which one needs to remove by a continuum extrapolation. As mentioned previously, in this respect the present method differs in principle from those in which α_s is determined from physical observables. In the general case, the numerical results of the lattice simulations at a value of μ fixed in physical units can be extrapolated to the continuum limit, and the result can be analyzed as to whether it shows perturbative running as a function of μ in the continuum. For observables at the cutoff-scale ($q^* = d/a$), discretization effects cannot easily be separated out from perturbation theory, as the scale for the coupling comes from the lattice spacing. Therefore the restriction $a\mu \ll 1$ (the 'continuum extrapolation' criterion) is not applicable here. Discretization errors of order a^2 are, however, present. Since $a \sim \exp(-1/(2b_0 g_0^2)) \sim \exp(-1/(8\pi b_0 \alpha(q^*))$, these errors now appear as power corrections to the perturbative running, and have to be taken into account in the study of the perturbative behaviour, which is to be verified by changing a. One thus usually fits with power corrections in this method.

In order to keep a symmetry with the 'continuum extrapolation' criterion for physical observables and to remember that discretization errors are, of course, relevant, we replace it here by one for the lattice spacings used:

- Lattice spacings
  - ★ 3 or more lattice spacings, at least 2 points below $a = 0.1\,\text{fm}$
  - ○ 2 lattice spacings, at least 1 point below $a = 0.1\,\text{fm}$
  - ■ otherwise

9.6.3 Discussion of computations

Note that due to $\mu \sim 1/a$ being relatively large the results easily have a ★ or ○ in the rating on renormalization scale.

The work of El-Khadra 92 [86] employs a 1-loop formula to relate $\alpha^{(0)}_{\overline{\rm MS}}(\pi/a)$ to the boosted coupling for three lattice spacings $a^{-1} = 1.15,\ 1.78,\ 2.43\,\text{GeV}$. (The lattice spacing is determined from the charmonium 1S-1P splitting.) They obtain $\Lambda^{(0)}_{\overline{\rm MS}} = 234\,\text{MeV}$, corresponding to $\alpha_{\rm eff} = \alpha^{(0)}_{\overline{\rm MS}}(\pi/a) \approx 0.15$ - 0.2. The work of Aoki 94 [87] calculates $\alpha^{(2)}_V$ and $\alpha^{(2)}_{\overline{\rm MS}}$ for a single lattice spacing $a^{-1} \sim 2\,\text{GeV}$ again determined from charmonium 1S-1P splitting in 2-flavour QCD. Using 1-loop perturbation theory with boosted coupling, they obtain $\alpha^{(2)}_V = 0.169$ and $\alpha^{(2)}_{\overline{\rm MS}} = 0.142$. Davies 94 [88] gives a determination of $\alpha_{\rm V}$ from the expansion

$$-\ln W_{11} \equiv \tfrac{4\pi}{3}\alpha^{(N_f)}_{\rm V}(3.41/a) \times [1 - (1.185 + 0.070N_f)\alpha^{(N_f)}_{\rm V}]\,, \tag{263}$$

neglecting higher-order terms. They compute the Υ spectrum in $N_f = 0,\ 2$ QCD for single lattice spacings at $a^{-1} = 2.57,\ 2.47\,\text{GeV}$ and obtain $\alpha_{\rm V}(3.41/a) \simeq 0.15,\ 0.18$ respectively. Extrapolating the inverse coupling linearly in N_f, a value of $\alpha^{(3)}_{\rm V}(8.3\,\text{GeV}) = 0.196(3)$ is obtained. SESAM 99 [89] follows a similar strategy, again for a single lattice spacing. They linearly extrapolated results for $1/\alpha^{(0)}_{\rm V}$, $1/\alpha^{(2)}_{\rm V}$ at a fixed scale of $9\,\text{GeV}$ to give $\alpha^{(3)}_{\rm V}$, which is then perturbatively converted to $\alpha^{(3)}_{\overline{\rm MS}}$. This finally gave $\alpha^{(5)}_{\overline{\rm MS}}(M_Z) = 0.1118(17)$. Wingate 95 [90] also follow this method. With the scale determined from the charmonium 1S-1P splitting for single lattice spacings in $N_f = 0,\ 2$ giving $a^{-1} \simeq 1.80\,\text{GeV}$ for $N_f = 0$ and $a^{-1} \simeq 1.66\,\text{GeV}$ for $N_f = 2$ they obtain $\alpha^{(0)}_{\rm V}(3.41/a) \simeq 0.15$ and $\alpha^{(2)}_{\rm V} \simeq 0.18$ respectively. Extrapolating the coupling linearly in N_f, they obtain $\alpha^{(3)}_{\rm V}(6.48\,\text{GeV}) = 0.194(17)$.

The QCDSF/UKQCD collaborations, QCDSF/UKQCD 05 [93], [94–96], use the 2-loop relation (re-written here in terms of α)

$$\frac{1}{\alpha_{\overline{\rm MS}}(\mu)} = \frac{1}{\alpha_{\rm P}(1/a)} + 4\pi(2b_0 \ln a\mu - t^P_1) + (4\pi)^2(2b_1 \ln a\mu - t^P_2)\alpha_{\rm P}(1/a)\,, \tag{264}$$

where t^P_1 and t^P_2 are known. (A 2-loop relation corresponds to a 3-loop lattice β-function.) This was used to directly compute $\alpha_{\overline{\rm MS}}$, and the scale was chosen so that the $\mathcal{O}(\alpha^0_{\rm P})$ term vanishes, i.e.

$$\mu^* = \frac{1}{a}\exp\left[t^P_1/(2b_0)\right] \approx \begin{cases} 2.63/a & N_f = 0 \\ 1.4/a & N_f = 2 \end{cases}\,. \tag{265}$$

The method is to first compute $\alpha_{\rm P}(1/a)$ and from this using Eq. (264) to find $\alpha_{\overline{\rm MS}}(\mu^*)$. The RG equation, Eq. (233), then determines $\mu^*/\Lambda_{\overline{\rm MS}}$ and hence using Eq. (265) leads to the result for $r_0\Lambda_{\overline{\rm MS}}$. This avoids giving the scale in MeV until the end. In the $N_f = 0$ case 7 lattice spacings were used [34], giving a range $\mu^*/\Lambda_{\overline{\rm MS}} \approx 24$ - 72 (or $a^{-1} \approx 2$ - $7\,\text{GeV}$) and $\alpha_{\rm eff} = \alpha_{\overline{\rm MS}}(\mu^*) \approx 0.15$ - 0.10. Neglecting higher-order perturbative terms (see discussion after Eq. (266) below) in Eq. (264) this is sufficient to allow a continuum extrapolation of $r_0\Lambda_{\overline{\rm MS}}$. A similar computation for $N_f = 2$ by QCDSF/UKQCD 05 [93] gave $\mu^*/\Lambda_{\overline{\rm MS}} \approx 12$ - 17 (or roughly $a^{-1} \approx 2$ - $3\,\text{GeV}$) and $\alpha_{\rm eff} = \alpha_{\overline{\rm MS}}(\mu^*) \approx 0.20$ - 0.18. The $N_f = 2$ results of QCDSF/UKQCD 05 [93] are affected by an uncertainty which was not known at the time of publication: It has been realized that the values of r_0/a of Ref. [93] were significantly too

Collaboration	Ref.	N_f	publication status	renormalization scale	perturbative behaviour	lattice spacings	scale	$\Lambda_{\overline{\rm MS}}$[MeV]	$r_0\Lambda_{\overline{\rm MS}}$
HPQCD 10[a §]	[91]	2+1	A	○	★	★	$r_1 = 0.3133(23)$ fm	340(9)	0.812(22)
HPQCD 08A[a]	[83]	2+1	A	○	★	★	$r_1 = 0.321(5)$ fm[††]	338(12)[⋆]	0.809(29)
Maltman 08[a]	[92]	2+1	A	○	○	★	$r_1 = 0.318$ fm	352(17)[†]	0.841(40)
HPQCD 05A[a]	[82]	2+1	A	○	○	○	r_1[††]	319(17)[⋆⋆]	0.763(42)
QCDSF/UKQCD 05	[93]	2	A	★	■	★	$r_0 = 0.467(33)$ fm	261(17)(26)	0.617(40)(21)[b]
SESAM 99[c]	[89]	2	A	○	■	■	$c\bar{c}$(1S-1P)		
Wingate 95[d]	[90]	2	A	★	■	■	$c\bar{c}$(1S-1P)		
Davies 94[e]	[88]	2	A	★	■	■	Υ		
Aoki 94[f]	[87]	2	A	★	■	■	$c\bar{c}$(1S-1P)		
FlowQCD 15	[11]	0	P	★	★	★	$w_{0.4} = 0.193(3)$ fm[i]	258(6)[i]	0.618(11)[i]
QCDSF/UKQCD 05	[93]	0	A	★	○	★	$r_0 = 0.467(33)$ fm	259(1)(20)	0.614(2)(5)[b]
SESAM 99[c]	[89]	0	A	★	■	■	$c\bar{c}$(1S-1P)		
Wingate 95[d]	[90]	0	A	★	■	■	$c\bar{c}$(1S-1P)		
Davies 94[e]	[88]	0	A	★	■	■	Υ		
El-Khadra 92[g]	[86]	0	A	★	■	○	$c\bar{c}$(1S-1P)	234(10)	0.560(24)[h]

[a] The numbers for Λ have been converted from the values for $\alpha_s^{(5)}(M_Z)$.

[§] $\alpha^{(3)}_{\overline{\rm MS}}(5\ {\rm GeV}) = 0.2034(21)$, $\alpha^{(5)}_{\overline{\rm MS}}(M_Z) = 0.1184(6)$, only update of intermediate scale and c-, b-quark masses, supersedes HPQCD 08A.

[†] $\alpha^{(5)}_{\overline{\rm MS}}(M_Z) = 0.1192(11)$.

[⋆] $\alpha_V^{(3)}(7.5\,{\rm GeV}) = 0.2120(28)$, $\alpha^{(5)}_{\overline{\rm MS}}(M_Z) = 0.1183(8)$, supersedes HPQCD 05.

[††] Scale is originally determined from Υ mass splitting. r_1 is used as an intermediate scale. In conversion to $r_0\Lambda_{\overline{\rm MS}}$, r_0 is taken to be 0.472 fm.

[⋆⋆] $\alpha_V^{(3)}(7.5\,{\rm GeV}) = 0.2082(40)$, $\alpha^{(5)}_{\overline{\rm MS}}(M_Z) = 0.1170(12)$.

[b] This supersedes Refs. [94–96]. $\alpha^{(5)}_{\overline{\rm MS}}(M_Z) = 0.112(1)(2)$. The $N_f = 2$ results were based on values for r_0/a which have later been found to be too small [29]. The effect will be of the order of 10–15%, presumably an increase in Λr_0.

[c] $\alpha^{(5)}_{\overline{\rm MS}}(M_Z) = 0.1118(17)$.

[d] $\alpha_V^{(3)}(6.48\,{\rm GeV}) = 0.194(7)$ extrapolated from $N_f = 0, 2$. $\alpha^{(5)}_{\overline{\rm MS}}(M_Z) = 0.107(5)$.

[e] $\alpha_P^{(3)}(8.2\,{\rm GeV}) = 0.1959(34)$ extrapolated from $N_f = 0, 2$. $\alpha^{(5)}_{\overline{\rm MS}}(M_Z) = 0.115(2)$.

[f] Estimated $\alpha^{(5)}_{\overline{\rm MS}}(M_Z) = 0.108(5)(4)$.

[g] This early computation violates our requirement that scheme conversions are done at the 2-loop level. $\Lambda^{(4)}_{\overline{\rm MS}} = 160(^{+47}_{-37})$MeV, $\alpha^{(4)}_{\overline{\rm MS}}(5{\rm GeV}) = 0.174(12)$. We converted this number to give $\alpha^{(5)}_{\overline{\rm MS}}(M_Z) = 0.106(4)$.

[h] We used $r_0 = 0.472$ fm to convert to $r_0\Lambda_{\overline{\rm MS}}$.

[i] Reference scale $w_{0.4}$ where w_x is defined by $t\partial_t[t^2\langle E(t)\rangle]\big|_{t=w_x^2} = x$ in terms of the action density $E(t)$ at positive flow time t [11]. Our conversion to r_0 scale using [11] $r_0/w_{0.4} = 2.587(45)$ and $r_0 = 0.472$ fm.

Table 47: Wilson loop results.

low [29]. As this effect is expected to depend on a, it influences the perturbative behaviour leading us to assign a ■ for that criterion.

Since FLAG 13, there has been one new result for $N_f = 0$ by FlowQCD 15 [11]. They also use the techniques as described in Eqs. (264), (265), but together with the gradient flow scale w_0 (rather than the r_0 scale). The continuum limit is estimated by extrapolating the data at 9 lattice spacings linearly in a^2. The data range used is $\mu^*/\Lambda_{\overline{\rm MS}} \approx 40$ - 120 (or $a^{-1} \approx 3$ - 11 GeV) and $\alpha_{\overline{\rm MS}}(\mu^*) \approx 0.12$ - 0.09. Since a very small value of $\alpha_{\overline{\rm MS}}$ is reached, there is a ★ in the perturbative behaviour. Note that our conversion to the common r_0 scale leads to a significant increase of the error of the Λ parameter compared to[7] $w_{0.4}\Lambda_{\overline{\rm MS}} = 0.2388(5)(13)$.

The work of HPQCD 05A [82] (which supersedes the original work [97]) uses three lattice spacings $a^{-1} \approx 1.2$, 1.6, 2.3 GeV for $2+1$ flavour QCD. Typically the renormalization scale $q \approx \pi/a \approx 3.50 - 7.10$ GeV, corresponding to $\alpha_{\rm V'} \approx 0.22 - 0.28$.

In the later update HPQCD 08A [83] twelve data sets (with six lattice spacings) are now used reaching up to $a^{-1} \approx 4.4$ GeV corresponding to $\alpha_{\rm V'} \approx 0.18$. The values used for the scale r_1 were further updated in HPQCD 10 [91]. Maltman 08 [92] uses most of the same lattice ensembles as HPQCD 08A [83], but considers a much smaller set of quantities (three versus 22) that are less sensitive to condensates. They also use different strategies for evaluating the condensates and for the perturbative expansion, and a slightly different value for the scale r_1. The central values of the final results from Maltman 08 [92] and HPQCD 08A [83] differ by 0.0009 (which would be decreased to 0.0007 taking into account a reduction of 0.0002 in the value of the r_1 scale used by Maltman 08 [92]).

As mentioned before, the perturbative coefficients are computed through 3-loop order [98], while the higher-order perturbative coefficients c_n with $n_{\rm max} \geq n > 3$ (with $n_{\rm max} = 10$) are numerically fitted using the lattice-simulation data for the lattice spacings with the help of Bayesian methods. It turns out that corrections in Eq. (260) are of order $|c_i/c_1|\alpha^i = 5$–15% and 3–10% for $i = 2, 3$, respectively. The inclusion of a fourth-order term is necessary to obtain a good fit to the data, and leads to a shift of the result by 1 – 2 sigma. For all but one of the 22 quantities, central values of $|c_4/c_1| \approx 2 - 4$ were found, with errors from the fits of ≈ 2.

An important source of uncertainty is the truncation of perturbation theory. In HPQCD 08A [83], 10 [91] it is estimated to be about 0.4% of $\alpha_{\overline{\rm MS}}(M_Z)$. In FLAG 13 we included a rather detailed discussion of the issue with the result that we prefer for the time being a more conservative error based on the above estimate $|c_4/c_1| = 2$. From Eq. (259) this gives an estimate of the uncertainty in $\alpha_{\rm eff}$ of

$$\Delta\alpha_{\rm eff}(\mu_1) = \left|\frac{c_4}{c_1}\right| \alpha^4_{\rm eff}(\mu_1)\,, \tag{266}$$

at the scale μ_1 where $\alpha_{\rm eff}$ is computed from the Wilson loops. This can be used with a variation in Λ at lowest order of perturbation theory and also applied to α_s evolved to a different scale μ_2[8],

$$\frac{\Delta\Lambda}{\Lambda} = \frac{1}{8\pi b_0 \alpha_s}\frac{\Delta\alpha_s}{\alpha_s}\,, \qquad \frac{\Delta\alpha_s(\mu_2)}{\Delta\alpha_s(\mu_1)} = \frac{\alpha_s^2(\mu_2)}{\alpha_s^2(\mu_1)}\,. \tag{267}$$

[7] The scale $w_{0.4}$ used in FlowQCD 15 [11] is a modified w_0 Wilson flow scale. With this notation $w_0 \equiv w_{0.3}$.

[8] From Eq. (238) we see that α_s is continuous and differentiable across the mass thresholds (at the same scale). Therefore to leading order α_s and $\Delta\alpha_s$ are independent of N_f.

We shall later use this with $\mu_2 = M_Z$ and $\alpha_s(\mu_1) = 0.2$ as a typical value extracted from Wilson loops in HPQCD 10 [91], HPQCD 08A [83].

Again we note that the results of QCDSF/UKQCD 05 [93] ($N_f = 0$) and FlowQCD 15 [11] may be affected by frozen topology as they have lattice spacings significantly below $a = 0.05\,\text{fm}$. The associated additional systematic error is presently unknown.

Tab. 47 summarizes the results.

9.7 α_s from current two-point functions

9.7.1 General considerations

The method has been introduced in Ref. [99] and updated in Ref. [91], see also Ref. [100]. Since FLAG 13 a new application, HPQCD 14A [12], with 2+1+1 flavours has appeared. There the definition for larger-n moments is somewhat simplified and we describe it here. The previously used one can be found in FLAG 13.

The basic observable is constructed from a current

$$J(x) = im_{0h}\overline{\psi}_h(x)\gamma_5\psi_{h'}(x) \tag{268}$$

of two mass-degenerate heavy-valence quarks, h, h'. The pre-factor m_{0h} denotes the bare mass of the quark. With a residual chiral symmetry, $J(x)$ is a renormalization group invariant local field, i.e. it requires no renormalization. Staggered fermions and twisted mass fermions have such a residual chiral symmetry. The (Euclidean) time-slice correlation function

$$G(x_0) = a^3 \sum_{\vec{x}} \langle J^\dagger(x) J(0)\rangle\,, \tag{269}$$

($J^\dagger(x) = im_{0h}\overline{\psi}_{h'}(x)\gamma_5\psi_h(x)$) has a $\sim x_0^{-3}$ singularity at short distances and moments

$$G_n = a \sum_{t=-(T/2-a)}^{T/2-a} t^n\, G(t)\,, \tag{270}$$

are nonvanishing for even n and furthermore finite for $n \geq 4$. Here T is the time extent of the lattice. The moments are dominated by contributions at t of order $1/m_{0h}$. For large mass m_{0h} these are short distances and the moments become increasingly perturbative for decreasing n. Denoting the lowest-order perturbation theory moments by $G_n^{(0)}$, one defines the normalized moments

$$\tilde{R}_n = \begin{cases} G_4/G_4^{(0)} & \text{for } n = 4\,, \\ \dfrac{G_n^{1/(n-4)}}{m_{0c}\left(G_n^{(0)}\right)^{1/(n-4)}} & \text{for } n \geq 6\,, \end{cases} \tag{271}$$

of even order n. Note that Eq. (268) contains the variable (bare) heavy-quark mass m_{0h}, while Eq. (271) is defined with the charm-quark mass, tuned to its physical value. The normalization $m_{0c}\left(G_n^{(0)}\right)^{1/(n-4)}$ in Eq. (271) ensures that $\tilde{R}_n$ remains renormalization group invariant, but introduces a mass scale. In the continuum limit the normalized moments can then be parameterized in terms of functions

$$\tilde{R}_n \equiv \begin{cases} r_4(\alpha_s(\mu)) & \text{for } n = 4\,, \\ \dfrac{r_n(\alpha_s(\mu))}{\bar{m}_c(\mu)} & \text{for } n \geq 6\,, \end{cases} \tag{272}$$

with $\bar{m}_c(\mu)$ being the renormalized charm-quark mass. The reduced moments r_n have a perturbative expansion

$$r_n = 1 + r_{n,1}\alpha_s + r_{n,2}\alpha_s^2 + r_{n,3}\alpha_s^3 + \dots , \tag{273}$$

where the written terms $r_{n,i}(\mu/\bar{m}_h(\mu))$, $i \le 3$ are known for low n from Refs. [101–105]. In practice, the expansion is performed in the $\overline{\rm MS}$ scheme. Matching nonperturbative lattice results for the moments to the perturbative expansion, one determines an approximation to $\alpha_{\overline{\rm MS}}(\mu)$ as well as $\bar{m}_c(\mu)$. With the lattice spacing (scale) determined from some extra physical input, this calibrates μ. As usual suitable pseudoscalar masses determine the bare quark masses, here in particular the charm mass, and then through Eq. (272) the renormalized charm-quark mass.

A difficulty with this approach is that large masses are needed to enter the perturbative domain. Lattice artefacts can then be sizeable and have a complicated form. The ratios in Eq. (271) use the tree-level lattice results in the usual way for normalization. This results in unity as the leading term in Eq. (273), suppressing some of the kinematical lattice artefacts. We note that in contrast to e.g. the definition of $\alpha_{\rm qq}$, here the cutoff effects are of order $a^k\alpha_s$, while there the tree-level term defines α_s and therefore the cutoff effects after tree-level improvement are of order $a^k\alpha_s^2$.

Finite-size effects (FSE) due to the omission of $|t| > T/2$ in Eq. (270) grow with n as $(m_{\rm p}T/2)^n \exp(-m_{\rm p}T/2)$. In practice, however, since the (lower) moments are short-distance dominated, the FSE are expected to be irrelevant at the present level of precision.

Moments of correlation functions of the quark's electromagnetic current can also be obtained from experimental data for e^+e^- annihilation [106, 107]. This enables a nonlattice determination of α_s using a similar analysis method. In particular, the same continuum perturbation theory computation enters both the lattice and the phenomenological determinations.

9.7.2 Discussion of computations

The method has originally been applied in HPQCD 08B [99] and in HPQCD 10 [91], based on the MILC ensembles with $2+1$ flavours of Asqtad staggered quarks and HISQ valence quarks. The scale was set using $r_1 = 0.321(5)\,$fm in HPQCD 08B [99] and the updated value $r_1 = 0.3133(23)\,$fm in HPQCD 10 [91]. The effective range of couplings used is here given for $n = 4$, which is the moment most dominated by short (perturbative) distances and important in the determination of α_s. The range is similar for other ratios. With $r_{4,1} = 0.7427$ and $R_4 = 1.28$ determined in the continuum limit at the charm mass in Ref. [99], we have $\alpha_{\rm eff} = 0.38$ at the charm-quark mass, which is the mass value where HPQCD 08B [99] carries out the analysis. In HPQCD 10 [91] a set of masses is used, with $R_4 \in [1.09, 1.29]$ which corresponds to $\alpha_{\rm eff} \in [0.12, 0.40]$.

The available data of HPQCD 10 [91] is summarized in the left panel of Fig. 31 where we plot $\alpha_{\rm eff}$ against $m_{\rm p}r_1$. For the continuum limit criterion, we choose the scale $\mu = 2\bar{m}_h \approx m_{\rm p}/1.1$, where we have taken $\bar{m}_h$ in the $\overline{\rm MS}$ scheme at scale $\bar{m}_h$ and the numerical value 1.1 was determined in HPQCD 10B [108].

The data in Fig. 31 are grouped according to the range of $a\mu$ that they cover. The vertical spread of the results for $\alpha_{\rm eff}$ at fixed $r_1 m_{\rm p}$ in the figure measures the discretization errors seen: in the continuum we would expect all the points to lie on one universal curve. The plots illustrate the selection applied by our criterion for the continuum limit with our choices for

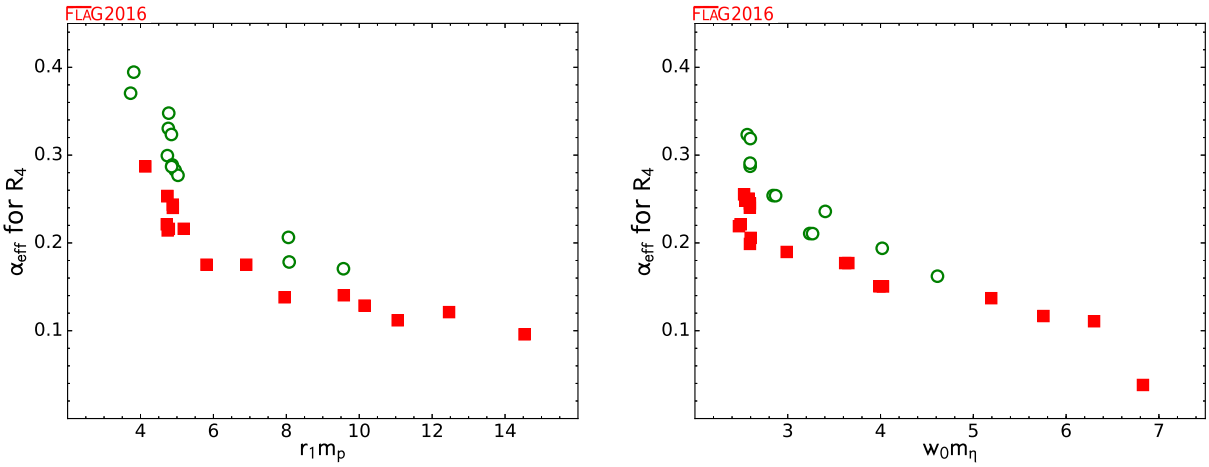

Figure 31: $\alpha_{\rm eff}$ for R_4 from HPQCD 10 data (left) and from HPQCD 14A (right). A similar graph for R_6/R_8 is shown in FLAG 13. Symbols correspond to ○ for data with $1 \leq a\mu \leq 1.5$ and ■ for $a\mu > 1.5$, while ★ ($a\mu < 1/2$) is not present. This corresponds exactly to the $a\mu$ part of our continuum limit criterion, but does not consider how many lattice spacings are present. Note that mistunings in the quark masses have not been accounted for, but, estimated as in HPQCD 14A [12], they are smaller than the size of the symbols in the graphs.

μ. Fig. 31 gives reason for concern, since it shows that the discretization errors that need to be removed in the continuum extrapolation are not small.

With our choices for μ, the continuum limit criterion is satisfied for 3 lattice spacings when $\alpha_{\rm eff} \leq 0.3$ and $n = 4$. Larger-n moments are more influenced by nonperturbative effects. For the n values considered, adding a gluon condensate term only changed error bars slightly in HPQCD's analysis. We note that HPQCD in their papers perform a global fit to all data using a joint expansion in powers of α_s^n, $(\Lambda/(m_{\rm p}/2))^j$ to parameterize the heavy-quark mass dependence, and $(am_{\rm p}/2)^{2i}$ to parameterize the lattice-spacing dependence. To obtain a good fit, they must exclude data with $am_{\rm p} > 1.95$ and include lattice-spacing terms a^{2i} with i greater than 10. Because these fits include many more fit parameters than data points, HPQCD uses their expectations for the sizes of coefficients as Bayesean priors. The fits include data with masses as large as $am_{\rm p}/2 \sim 0.86$, so there is only minimal suppression of the many high-order contributions for the heavier masses. It is not clear, however, how sensitive the final results are to the larger $am_{\rm p}/2$ values in the data. The continuum limit of the fit is in agreement with a perturbative scale dependence (a 5-loop running $\alpha_{\overline{\rm MS}}$ with a fitted 5-loop coefficient in the β-function is used). Indeed, Fig. 2 of Ref. [91] suggests that HPQCD's fit describes the data well.

The new computation, HPQCD 14A [12], is based on MILC's 2+1+1 HISQ staggered ensembles. Compared to HPQCD 10 [91] valence- and sea-quarks now use the same discretization and the scale is set through the gradient flow scale w_0, determined to $w_0 = 0.1715(9)$ fm in Ref. [109].

We again show the values of $\alpha_{\rm eff}$ as a function of the physical scale. Discretization errors are noticeable. A number of data points, satisfy our continuum limit criterion $a\mu < 1.5$, at two different lattice spacings. This does not by itself lead to a ○ but the next-larger lattice

spacing does not miss the criterion by much, see Tab. **??**. We therefore assign a ○ in that criterion.

The other details of the analysis by HPQCD 10 [91] are very similar to the ones described above, with one noteworthy exception. The new definition of the moments does not involve the pseudoscalar $h\bar{h}$ mass anymore. Therefore its relation to the quark mass does not need to be modeled in the fit. Since it is now replaced by the renormalized charm-quark mass, the analysis produces a result for α_s and the charm-quark mass at the same time. Here we only discuss the result for α_s.

In Tab. 48 we list the current two-point function results. Thus far, only one group has used

Collaboration	Ref.	N_f	publication status	renormalization scale	perturbative behaviour	continuum extrapolation	scale	$\Lambda_{\overline{\rm MS}}$[MeV]	$r_0\Lambda_{\overline{\rm MS}}$
HPQCD 14A	[12]	2+1+1	A	○	★	○	$w_0 = 0.1715(9)\,\text{fm}^a$	$294(11)^{bc}$	0.703(26)
HPQCD 10	[91]	2+1	A	○	★	○	$r_1 = 0.3133(23)\,\text{fm}^\dagger$	$338(10)^\star$	0.809(25)
HPQCD 08B	[99]	2+1	A	■	■	■	$r_1 = 0.321(5)\,\text{fm}^\dagger$	$325(18)^+$	0.777(42)

[a] Scale determined in [110] using f_π.
[b] $\alpha^{(4)}_{\overline{\rm MS}}(5\,\text{GeV}) = 0.2128(25)$, $\alpha^{(5)}_{\overline{\rm MS}}(M_Z) = 0.11822(74)$.
[c] Our conversion for $\Lambda_{\overline{\rm MS}}$ for $N_f = 4$. We also used $r_0 = 0.472\,\text{fm}$.
[†] Scale is determined from Υ mass splitting.
[⋆] $\alpha^{(3)}_{\overline{\rm MS}}(5\,\text{GeV}) = 0.2034(21)$, $\alpha^{(5)}_{\overline{\rm MS}}(M_Z) = 0.1183(7)$.
[+] $\alpha^{(4)}_{\overline{\rm MS}}(3\,\text{GeV}) = 0.251(6)$, $\alpha^{(5)}_{\overline{\rm MS}}(M_Z) = 0.1174(12)$.

Table 48: Current two-point function results.

this approach, which models complicated and potentially large cutoff effects together with a perturbative coefficient. We therefore are waiting to see confirmation by other collaborations of the small systematic errors obtained (cf. discussion in Sec. 9.9.2). (We note that more investigations of this method are in progress [111].) We do, however, include the values of $\alpha_{\overline{\rm MS}}(M_Z)$ and $\Lambda_{\overline{\rm MS}}$ of HPQCD 10 [91] and HPQCD 14A [12] in our final range.

9.8 α_s from QCD vertices

9.8.1 General considerations

The most intuitive and in principle direct way to determine the coupling constant in QCD is to compute the appropriate three- or four-point gluon vertices or alternatively the quark-quark-gluon vertex or ghost-ghost-gluon vertex (i.e. $q\bar{q}A$ or $c\bar{c}A$ vertex respectively). A suitable combination of renormalization constants then leads to the relation between the bare (lattice) and renormalized coupling constant. This procedure requires the implementation of a nonperturbative renormalization condition and the fixing of the gauge. For the study of

nonperturbative gauge fixing and the associated Gribov ambiguity, we refer to Refs. [112–114] and references therein. In practice the Landau gauge is used and the renormalization constants are defined by requiring that the vertex is equal to the tree level value at a certain momentum configuration. The resulting renormalization schemes are called 'MOM' scheme (symmetric momentum configuration) or '$\widetilde{\text{MOM}}$' (one momentum vanishes), which are then converted perturbatively to the $\overline{\text{MS}}$ scheme.

A pioneering work to determine the three-gluon vertex in the $N_f = 0$ theory is Alles 96 [115] (which was followed by Ref. [116] for two flavour QCD); a more recent $N_f = 0$ computation was Ref. [117] in which the three-gluon vertex as well as the ghost-ghost-gluon vertex was considered. (This requires in general a computation of the propagator of the Faddeev–Popov ghost on the lattice.) The latter paper concluded that the resulting $\Lambda_{\overline{\text{MS}}}$ depended strongly on the scheme used, the order of perturbation theory used in the matching and also on nonperturbative corrections [118].

Subsequently in Refs. [119, 120] a specific $\widetilde{\text{MOM}}$ scheme with zero ghost momentum for the ghost-ghost-gluon vertex was used. In this scheme, dubbed the 'MM' (Minimal MOM) or 'Taylor' (T) scheme, the vertex is not renormalized, and so the renormalized coupling reduces to

$$\alpha_{\text{T}}(\mu) = D^{\text{gluon}}_{\text{lat}}(\mu, a) D^{\text{ghost}}_{\text{lat}}(\mu, a)^2 \, \frac{g_0^2(a)}{4\pi} \,, \tag{274}$$

where $D^{\text{ghost}}_{\text{lat}}$ and $D^{\text{gluon}}_{\text{lat}}$ are the (bare lattice) dressed ghost and gluon 'form factors' of these propagator functions in the Landau gauge,

$$D^{ab}(p) = -\delta^{ab} \, \frac{D^{\text{ghost}}(p)}{p^2} \,, \qquad D^{ab}_{\mu\nu}(p) = \delta^{ab} \left(\delta_{\mu\nu} - \frac{p_\mu p_\nu}{p^2} \right) \frac{D^{\text{gluon}}(p)}{p^2} \,, \tag{275}$$

and we have written the formula in the continuum with $D^{\text{ghost/gluon}}(p) = D^{\text{ghost/gluon}}_{\text{lat}}(p, 0)$. Thus there is now no need to compute the ghost-ghost-gluon vertex, just the ghost and gluon propagators.

9.8.2 Discussion of computations

For the calculations considered here, to match to perturbative scaling, it was first necessary to reduce lattice artifacts by an $H(4)$ extrapolation procedure (addressing $O(4)$ rotational invariance), e.g. ETM 10F [126] or by lattice perturbation theory, e.g. Sternbeck 12 [124]. To match to perturbation theory, collaborations vary in their approach. In ETM 10F [126] it was necessary to include the operator A^2 in the OPE of the ghost and gluon propagators, while in Sternbeck 12 [124] very large momenta are used and a^2p^2 and a^4p^4 terms are included in their fit to the momentum dependence. A further later refinement was the introduction of higher nonperturbative OPE power corrections in ETM 11D [123] and ETM 12C [122]. Although the expected leading power correction, $1/p^4$, was tried, ETM finds good agreement with their data only when they fit with the next-to-leading-order term, $1/p^6$. The update ETM 13D [121] investigates this point in more detail, using better data with reduced statistical errors. They find that after again including the $1/p^6$ term they can describe their data over a large momentum range from about 1.75 GeV to 7 GeV.

In all calculations except for Sternbeck 10 [125], Sternbeck 12 [124] , the matching with the perturbative formula is performed including power corrections in the form of condensates, in

Collaboration	Ref.	N_f	publication status	renormalization scale	perturbative behaviour	continuum extrapolation	scale	$\Lambda_{\overline{\rm MS}}$[MeV]	$r_0\Lambda_{\overline{\rm MS}}$
ETM 13D	[121]	2+1+1	A	○	○	■	f_π	$314(7)(14)(10)^{\S}$	$0.752(18)(34)(81)^{\dagger}$
ETM 12C	[122]	2+1+1	A	○	○	■	f_π	$324(17)^{\S}$	$0.775(41)^{\dagger}$
ETM 11D	[123]	2+1+1	A	○	○	■	f_π	$316(13)(8)(^{+0}_{-9})^{\star}$	$0.756(31)(19)(^{+0}_{-22})^{\dagger}$
Sternbeck 12	[124]	2+1	C				only running of α_s in Fig. 4		
Sternbeck 12	[124]	2	C				Agreement with $r_0\Lambda_{\overline{\rm MS}}$ value of [29]		
Sternbeck 10	[125]	2	C	○	★	■		$251(15)^{\#}$	0.60(3)(2)
ETM 10F	[126]	2	A	○	○	○	f_π	$330(23)(22)(^{+0}_{-33})$	$0.72(5)^{+}$
Boucaud 01B	[116]	2	A	○	○	■	$K^* - K$	$264(27)^{\star\star}$	0.669(69)
Sternbeck 12	[124]	0	C				Agreement with $r_0\Lambda_{\overline{\rm MS}}$ value of [72]		
Sternbeck 10	[125]	0	C	★	★	■		$259(4)^{\#}$	0.62(1)
Ilgenfritz 10	[127]	0	A	★	★	■	only running of α_s in Fig. 13		
Boucaud 08	[120]	0	A	○	★	■	$\sqrt{\sigma} = 445\,$MeV	$224(3)(^{+8}_{-5})$	$0.59(1)(^{+2}_{-1})$
Boucaud 05	[117]	0	A	■	★	■	$\sqrt{\sigma} = 445\,$MeV	320(32)	0.85(9)
Soto 01	[128]	0	A	○	○	○	$\sqrt{\sigma} = 445\,$MeV	260(18)	0.69(5)
Boucaud 01A	[129]	0	A	○	○	○	$\sqrt{\sigma} = 445\,$MeV	233(28) MeV	0.62(7)
Boucaud 00B	[130]	0	A	○	○	○		only running of α_s	
Boucaud 00A	[131]	0	A	○	○	○	$\sqrt{\sigma} = 445\,$MeV	$237(3)(^{+\ 0}_{-10})$	$0.63(1)(^{+0}_{-3})$
Becirevic 99B	[132]	0	A	○	○	■	$\sqrt{\sigma} = 445\,$MeV	$319(14)(^{+10}_{-20})$	$0.84(4)(^{+3}_{-5})$
Becirevic 99A	[133]	0	A	○	○	■	$\sqrt{\sigma} = 445\,$MeV	$\lesssim 353(2)(^{+25}_{-15})$	$\lesssim 0.93(^{+7}_{-4})$
Boucaud 98B	[134]	0	A	■	○	■	$\sqrt{\sigma} = 445\,$MeV	295(5)(15)	0.78(4)
Boucaud 98A	[135]	0	A	■	○	■	$\sqrt{\sigma} = 445\,$MeV	300(5)	0.79(1)
Alles 96	[115]	0	A	■	■	■	$\sqrt{\sigma} = 440\,$MeV^{++}	340(50)	0.91(13)

† We use the 2+1 value $r_0 = 0.472$ fm.
§ $\alpha^{(5)}_{\overline{\rm MS}}(M_Z) = 0.1200(14)$.
* First error is statistical; second is due to the lattice spacing and third is due to the chiral extrapolation. $\alpha^{(5)}_{\overline{\rm MS}}(M_Z) = 0.1198(9)(5)(^{+0}_{-5})$.
$^{\#}$ In the paper only $r_0\Lambda_{\overline{\rm MS}}$ is given, we converted to MeV with $r_0 = 0.472$ fm.
$^{+}$ The determination of r_0 from the f_π scale is found in Ref. [27].
** $\alpha^{(5)}_{\overline{\rm MS}}(M_Z) = 0.113(3)(4)$.
$^{++}$ The scale is taken from the string tension computation of Ref. [73].

Table 49: Results for the gluon–ghost vertex.

particular $\langle A^2\rangle$. Three lattice spacings are present in almost all calculations with $N_f = 0$, 2, but the scales ap are rather large. This mostly results in a ■ on the continuum extrapolation (Sternbeck 10 [125], Boucaud 01B [116] for $N_f = 2$. Ilgenfritz 10 [127], Boucaud 08 [120], Boucaud 05 [117], Becirevic 99B [132], Becirevic 99A [133], Boucaud 98B [134], Boucaud 98A [135], Alles 96 [115] for $N_f = 0$). A ○ is reached in the $N_f = 0$ computations Boucaud

00A [131], 00B [130], 01A [129], Soto 01 [128] due to a rather small lattice spacing, but this is done on a lattice of a small physical size. The $N_f = 2+1+1$ calculation, fitting with condensates, is carried out for two lattice spacings and with $ap > 1.5$, giving ■ for the continuum extrapolation as well. In ETM 10F [126] we have $0.25 < \alpha_{\rm eff} < 0.4$, while in ETM 11D [123], ETM 12C [122] (and ETM 13 [136]) we find $0.24 < \alpha_{\rm eff} < 0.38$ which gives a green circle in these cases for the renormalization scale. In ETM 10F [126] the values of ap violate our criterion for a continuum limit only slightly, and we give a ○.

In Sternbeck 10 [125], the coupling ranges over $0.07 \leq \alpha_{\rm eff} \leq 0.32$ for $N_f = 0$ and $0.19 \leq \alpha_{\rm eff} \leq 0.38$ for $N_f = 2$ giving ★ and ○ for the renormalization scale respectively. The fit with the perturbative formula is carried out without condensates, giving a satisfactory description of the data. In Boucaud 01A [129], depending on a, a large range of $\alpha_{\rm eff}$ is used which goes down to 0.2 giving a ○ for the renormalization scale and perturbative behaviour, and several lattice spacings are used leading to ○ in the continuum extrapolation. The $N_f = 2$ computation Boucaud 01B [129], fails the continuum limit criterion because both $a\mu$ is too large and an unimproved Wilson fermion action is used. Finally in the conference proceedings Sternbeck 12 [124], the $N_f = 0, 2, 3$ coupling $\alpha_{\rm T}$ is studied. Subtracting 1-loop lattice artefacts and subsequently fitting with a^2p^2 and a^4p^4 additional lattice artefacts, agreement with the perturbative running is found for large momenta ($r_0^2p^2 > 600$) without the need for power corrections. In these comparisons, the values of $r_0\Lambda_{\overline{\rm MS}}$ from other collaborations are used. As no numbers are given, we have not introduced ratings for this study.

In Tab. 49 we summarize the results. Presently there are no $N_f \geq 3$ calculations of α_s from QCD vertices that satisfy the FLAG criteria to be included in the range.

9.9 Summary

9.9.1 The present situation

We first summarize the status of lattice-QCD calculations of the QCD scale $\Lambda_{\overline{\rm MS}}$. Fig. 32 shows all results for $r_0\Lambda_{\overline{\rm MS}}$ discussed in the previous sections.

Many of the numbers are the ones given directly in the papers. However, when only $\Lambda_{\overline{\rm MS}}$ in physical units (MeV) is available, we have converted them by multiplying with the value of r_0 in physical units. The notation used is full green squares for results used in our final average, while a lightly shaded green square indicates that there are no red squares in the previous colour coding but the computation does not enter the ranges because either it has been superseded by an update or it is not published. Red open squares mean that there is at least one red square in the colour coding.

For $N_f = 0$ there is relatively little spread in the more recent numbers, even in those which do not satisfy our criteria.

When two flavours of quarks are included, the numbers extracted by the various groups show a considerable spread, as in particular older computations did not yet control the systematics sufficiently. This illustrates the difficulty of the problem and emphasizes the need for strict criteria. The agreement among the more modern calculations with three or more flavours, however, is quite good.

We now turn to the status of the essential result for phenomenology, $\alpha^{(5)}_{\overline{\rm MS}}(M_Z)$. In Tab. 50 and Fig. 33 we show all the results for $\alpha^{(5)}_{\overline{\rm MS}}(M_Z)$ (i.e. $\alpha_{\overline{\rm MS}}$ at the Z mass) obtained from $N_f = 2+1$ and $N_f = 2+1+1$ simulations. For comparison, we also include results from $N_f = 0, 2$ simulations, which are not relevant for phenomenology. For the $N_f \geq 3$ simulations,

Collaboration	Ref.	N_f	publication status	renormalization scale	perturbative behaviour	continuum extrapolation	$\alpha_{\overline{\rm MS}}(M_{\rm Z})$	Method	Table
HPQCD 14A	[12]	2+1+1	A	○	★	○	0.11822(74)	current two points	48
ETM 13D	[121]	2+1+1	A	○	○	■	0.1196(4)(8)(16)	gluon-ghost vertex	49
ETM 12C	[122]	2+1+1	A	○	○	■	0.1200(14)	gluon-ghost vertex	49
ETM 11D	[123]	2+1+1	A	○	○	■	$0.1198(9)(5)(^{+0}_{-5})$	gluon-ghost vertex	49
Bazavov 14	[10]	2+1	A	○	★	○	$0.1166(^{+12}_{-8})$	Q-$\bar{Q}$ potential	45
Bazavov 12	[70]	2+1	A	○	○	○	$0.1156(^{+21}_{-22})$	Q-$\bar{Q}$ potential	45
HPQCD 10	[91]	2+1	A	○	★	○	0.1183(7)	current two points	48
HPQCD 10	[91]	2+1	A	○	★	★	0.1184(6)	Wilson loops	47
JLQCD 10	[79]	2+1	A	■	■	■	$0.1118(3)(^{+16}_{-17})$	vacuum polarization	46
PACS-CS 09A	[53]	2+1	A	★	★	○	$0.118(3)^{\#}$	Schrödinger functional	44
Maltman 08	[92]	2+1	A	○	○	★	0.1192(11)	Wilson loops	47
HPQCD 08B	[99]	2+1	A	■	■	■	0.1174(12)	current two points	48
HPQCD 08A	[83]	2+1	A	○	★	★	0.1183(8)	Wilson loops	47
HPQCD 05A	[82]	2+1	A	○	○	○	0.1170(12)	Wilson loops	47
QCDSF/UKQCD 05	[93]	$0, 2 \to 3$	A	★	■	★	0.112(1)(2)	Wilson loops	47
Boucaud 01B	[116]	$2 \to 3$	A	○	○	■	0.113(3)(4)	gluon-ghost vertex	49
SESAM 99	[89]	$0, 2 \to 3$	A	★	■	■	0.1118(17)	Wilson loops	47
Wingate 95	[90]	$0, 2 \to 3$	A	★	■	■	0.107(5)	Wilson loops	47
Davies 94	[88]	$0, 2 \to 3$	A	★	■	■	0.115(2)	Wilson loops	47
Aoki 94	[87]	$2 \to 3$	A	★	■	■	0.108(5)(4)	Wilson loops	47
El-Khadra 92	[86]	$0 \to 3$	A	★	■	○	0.106(4)	Wilson loops	47

$^{\#}$ Result with a linear continuum extrapolation in a.

Table 50: Results for $\alpha_{\overline{\rm MS}}(M_{\rm Z})$. $N_f = 3$ results are matched at the charm and bottom thresholds and scaled to M_Z to obtain the $N_f = 5$ result. The arrows in the N_f column indicates which N_f ($N_f = 0$, 2 or a combination of both) were used to first extrapolate to $N_f = 3$ or estimate the $N_f = 3$ value through a model/assumption. The exact procedures used vary and are given in the various papers.

the conversion from $N_f = 3$ or $N_f = 4$ to $N_f = 5$ is made by matching the coupling constant at the charm and bottom quark thresholds and using the scale as determined or used by the authors. For $N_f = 0$, 2 the results for $\alpha_{\overline{\rm MS}}$ in the summary table come from evaluations of $\alpha_{\overline{\rm MS}}$ at a relatively low scale and are extrapolated in N_f to $N_f = 3$.

As can be seen from the tables and figures, at present there are several computations satisfying the criteria to be included in the FLAG average. Since FLAG 13 two new computations of $\alpha^{(5)}_{\overline{\rm MS}}(M_Z)$, Bazavov 14 [10] and HPQCD 14A [12], pass all our criteria with a ○. We note that none of those calculations of $\alpha^{(5)}_{\overline{\rm MS}}(M_Z)$ satisfy all of our more stringent criteria: a ★ for

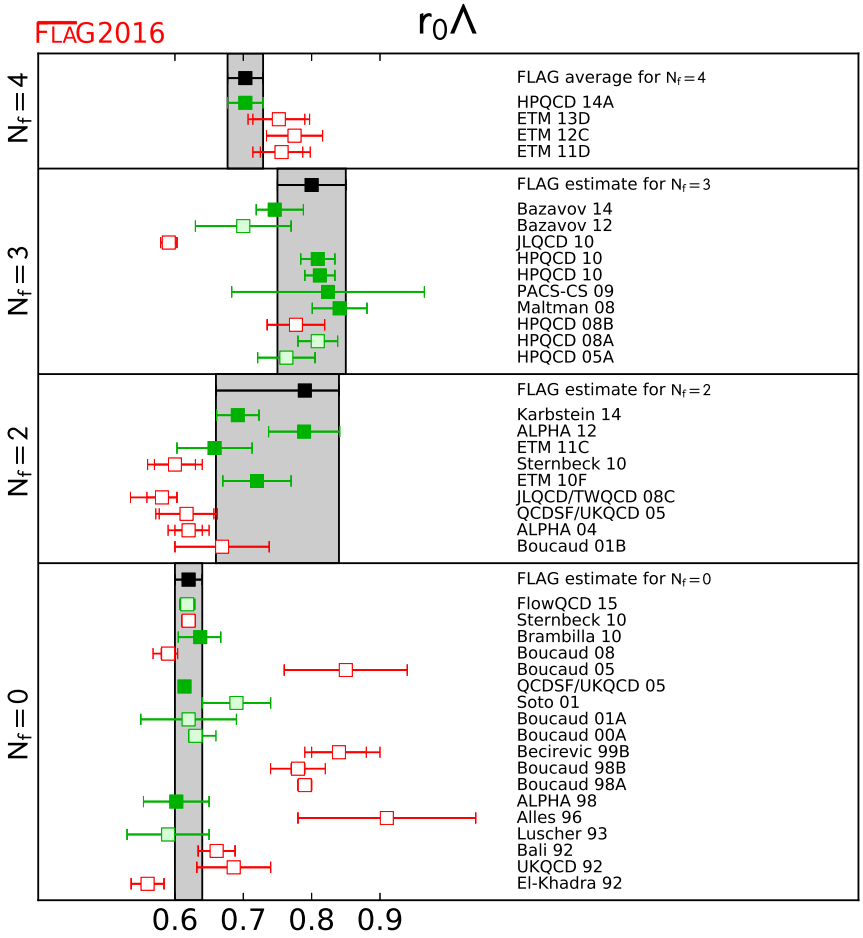

Figure 32: $r_0\Lambda_{\overline{\rm MS}}$ estimates for $N_f = 0$, 2, 3, 4 flavours. Full green squares are used in our final ranges, pale green squares also indicate that there are no red squares in the colour coding but the computations were superseded by later more complete ones or not published, while red open squares mean that there is at least one red square in the colour coding.

the renormalization scale, perturbative behaviour and continuum extrapolation. The results, however, are obtained from four different methods that have different associated systematics, and agree quite well within the stated uncertainties.

9.9.2 Our range for $\alpha^{(5)}_{\overline{\rm MS}}$

We now explain the determination of our range. We only include those results without a red tag and that are published in a refereed journal. We also do not include any numbers which were obtained by extrapolating from theories with less than three flavours. There is no real basis for such extrapolations; rather they use ad hoc assumptions on the low-energy behaviour of the theories. One also notices from the published results that the estimated numbers are quite significantly below those with at least 2+1 flavours.

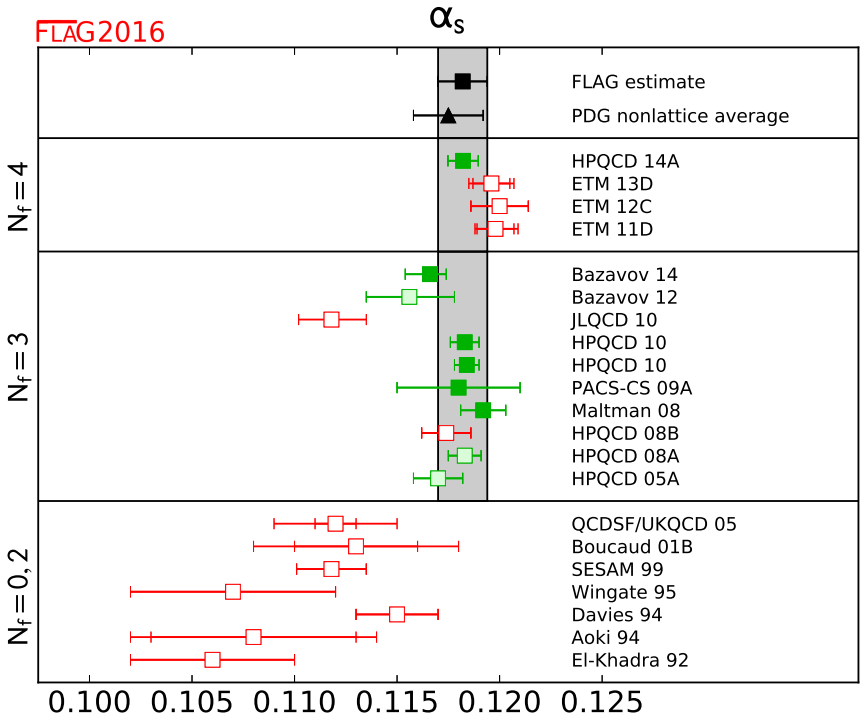

Figure 33: $\alpha^{(5)}_{\overline{\rm MS}}(M_Z)$, the coupling constant in the $\overline{\rm MS}$ scheme at the Z mass. The results labeled $N_f = 0, 2$ use estimates for $N_f = 3$ obtained by first extrapolating in N_f from $N_f = 0, 2$ results. Since this is not a theoretically justified procedure, these are not included in our final estimate and are thus given a red symbol. However, they are shown to indicate the progress made since these early calculations. The PDG entry indicates the outcome of their analysis excluding lattice results (see section 9.9.4).

A general issue with most recent determinations of $\alpha_{\overline{\rm MS}}$, both lattice and nonlattice, is that they are dominated by perturbative truncation errors, which are difficult to estimate. Further, all results discussed here except for those of Secs. 9.3, 9.6 are based on extractions of $\alpha_{\overline{\rm MS}}$ that are largely influenced by data with $\alpha_{\rm eff} \geq 0.3$. At smaller α_s the momentum scale μ quickly is at or above a^{-1}. We have included computations using $a\mu$ up to 1.5 and $\alpha_{\rm eff}$ up to 0.4, but one would ideally like to be significantly below that. Accordingly we choose at this stage to estimate the error ranges in a conservative manner, and not simply perform weighted averages with the individual errors estimated by each group.

Many of the methods have thus far only been applied by a single collaboration, and with simulation parameters that could still be improved. We therefore think that the following aspects of the individual calculations are important to keep in mind, and look forward to additional clarification and/or corroboration in the future.

• The potential computations Brambilla 10 [72], ETM 11C [71] and Bazavov 12 [70] give evidence that they have reached distances where perturbation theory can be used. However, in addition to Λ, a scale is introduced into the perturbative prediction by the process of

subtracting the renormalon contribution. This subtraction is avoided in Bazavov 14 [10] by using the force and again agreement with perturbative running is reported. The extractions of Λ are dominated by data with $\alpha_{\rm eff} \geq 0.3$. In contrast, Ref. [74], which studies the force instead of the potential and therefore does not need a renormalon subtraction, finds that significantly smaller lattice spacings would be needed in order for perturbation theory to be reliable in a region of $\mu = 1/r$ where discretization errors are controlled. Further study is still needed to clarify the situation.

• In the determination of α_s from observables at the lattice spacing scale, there is an interplay of higher-order perturbative terms and lattice artefacts. In HPQCD 05A [82], HPQCD 08A [83] and Maltman 08 [92] both lattice artifacts (which are power corrections in this approach) and higher-order perturbative terms are fitted. We note that, Maltman 08 [92] and HPQCD 08A [83] analyze largely the same data set but use different versions of the perturbative expansion and treatments of nonperturbative terms. After adjusting for the slightly different lattice scales used, the values of $\alpha_{\overline{\rm MS}}(M_Z)$ differ by 0.0004 to 0.0008 for the three quantities considered. In fact the largest of these differences (0.0008) comes from a tadpole-improved loop, which is expected to be best behaved perturbatively.

• Other computations with very small errors are HPQCD 10 [91] and HPQCD 14A [12], where correlation functions of heavy quarks are used to construct short-distance quantities. Due to the large quark masses needed to reach the region of small coupling, considerable discretization errors are present, see Fig. 31. These are treated by fits to the perturbative running (a 5-loop running $\alpha_{\overline{\rm MS}}$ with a fitted 5-loop coefficient in the β-function is used) with high-order terms in a double expansion in $a^2\Lambda^2$ and $a^2 m_{\rm h}^2$ supplemented by priors which limit the size of the coefficients. The priors play an especially important role in these fits given the much larger number of fit parameters than data points. We note, however, that the size of the coefficients does not prevent high-order terms from contributing significantly, since the data includes values of $am_{\rm p}/2$ that are rather close to 1.

As previously mentioned $\alpha^{(5)}_{\overline{\rm MS}}(M_Z)$ is summarized in Tab. 50 and Fig. 33. A number of calculations that include at least the effect of the strange quark make up our final estimate. These are Bazavov 14 [10], HPQCD 14A [12], HPQCD 10 [91] (Wilson loops and current two-point correlators), PACS-CS 09A [53], Maltman 08 [92] while HPQCD 08A/05A [82, 83] and Bazavov 12 [70] have been superseded by more recent calculations. We obtain the central value for our range,

$$\alpha^{(5)}_{\overline{\rm MS}}(M_Z) = 0.1182(12)\,, \tag{276}$$

from the weighted average of the six results.[9] Of the results that enter our range, those from Wilson loops (HPQCD 10 [91], and Maltman 08 [92]) and current two-point correlators (HPQCD 10 [91]) presently have the smallest quoted errors. We have just listed reasons to be careful in estimating the present overall uncertainty. We therefore take a larger range for $\alpha^{(5)}_{\overline{\rm MS}}(M_Z)$ than one would obtain from the weighted average, or even from the most precise individual calculation. We arrive at its value as follows. We make a conservative estimate of the perturbative uncertainty in the calculation of α_s from small Wilson loops. One approach for making such an estimate would be to take the largest of the differences between the calculations of Maltman 08 [92] and HPQCD 08A [83], 0.0008, which comes from the quantity computed by both groups that is expected to be best behaved perturbatively.

[9] We have symmetrized the asymmetric error bars of Bazavov 14 [10] to 0.1166(10) in taking the average.

This is somewhat larger than some of the estimates in the individual papers. Our choice is instead to take an estimate of the perturbative truncation error as the overall uncertainty. As explained in Sec. 9.6 the first unknown coefficient in the perturbative series was estimated in the fits to be $|c_4/c_1| \approx 2$. Using it in Eqs. (266,267) [10] yields $\Delta\alpha^{(5)}_{\overline{\rm MS}}(M_Z) = 0.0012$. This is larger than the estimate of 0.0008 above and is what we adopt as the uncertainty of the Wilson loop results. The second number with small errors entering the average comes from the analysis of moments of heavy quark correlators. Here an independent estimate of the uncertainty due to the fit to the a-dependence (see Fig. 31) is much more difficult to make; as discussed above, and in the absence of confirmation by other groups, we are not yet ready to use the result of HPQCD 10 [91] from the analysis of moments to reduce the size of our range. Thus the overall size of the range is determined by our estimate of the uncertainty of $\alpha^{(5)}_{\overline{\rm MS}}(M_Z)$ from Wilson loops. It is further reassuring to see that almost all central values that qualify for averaging are within the so-determined range.

The range for $\alpha^{(5)}_{\overline{\rm MS}}(M_Z)$ presented here is based on results with rather different systematics (apart from the matching across the charm threshold). We therefore believe that the true value is quite likely to lie within this range.

We emphasize once more that all computations which enter this range rely on a perturbative inclusion of the charm and beauty quarks. While perturbation theory for the matching of $\bar{g}^2_{N_f}$ and $\bar{g}^2_{N_f-1}$ looks very well behaved even at the mass of the charm, this scale is rather low and we have no accurate information about the precision of perturbation theory. Non-perturbative studies are not yet precise enough [137]. However, it seems unlikely that the associated uncertainty is comparable with the present errors. With future improved precision, this will become a relevant issue. Note that this uncertainty is also present in some of the phenomenological determinations, in particular from τ decays.

9.9.3 Ranges for $[r_0\Lambda]^{(N_f)}$ and $\Lambda_{\overline{\rm MS}}$

In the present situation, we give ranges for $[r_0\Lambda]^{(N_f)}$ and $\Lambda_{\overline{\rm MS}}$, discussing their determination case by case. We include results with $N_f < 3$ because it is interesting to see the N_f-dependence of the connection of low- and high-energy QCD. This aids our understanding of the field theory and helps in finding possible ways to tackle it beyond the lattice approach. It is also of interest in providing an impression on the size of the vacuum polarization effects of quarks, in particular with an eye on the still difficult-to-treat heavier charm and beauty quarks. Even if this information is rather qualitative, it may be valuable, given that it is of a completely nonperturbative nature. We emphasize that results for $[r_0\Lambda]^{(0)}$ and $[r_0\Lambda]^{(2)}$ are *not* meant to be used in phenomenology.

For $N_f = 2+1+1$, we presently do not quote a range as there is a single result: HPQCD 14A [12] found $[r_0\Lambda]^{(4)} = 0.70(3)$.

For $N_f = 2+1$, we take as a central value the weighted average of Bazavov 14 [10], HPQCD 10 [91] (Wilson loops and current two-point correlators), PACS-CS 09A [53] and Maltman 08 [92]. Since the uncertainty in r_0 is small compared to that of Λ, we can directly propagate the error from Eq. (276) and arrive at

$$[r_0\Lambda_{\overline{\rm MS}}]^{(3)} = 0.80(5)\,. \tag{277}$$

[10] More precisely, we use $\alpha^{(3)}_{\overline{\rm MS}}(5\,{\rm GeV}) = 0.203$ corresponding to Eq. (278) and $\alpha^{(5)}_{\overline{\rm MS}}(M_{\rm Z}) = 0.1182$ in Eqs. (266,267).

It is in good agreement with all 2+1 results without red tags. In physical units, using $r_0 = 0.472$ fm and neglecting its error, this means

$$\Lambda^{(3)}_{\overline{\rm MS}} = 336(19)\,{\rm MeV}\,. \tag{278}$$

For $N_f = 2$, at present there is one computation with a ★ rating for all criteria, ALPHA 12 [29]. We adopt it as our central value and enlarge the error to cover the central values of the other three results with filled green boxes. This results in an asymmetric error. Our range is unchanged as compared to FLAG 13,

$$[r_0\Lambda_{\overline{\rm MS}}]^{(2)} = 0.79(^{+\,5}_{-13})\,, \tag{279}$$

and in physical units, using $r_0 = 0.472$fm,

$$\Lambda^{(2)}_{\overline{\rm MS}} = 330(^{+21}_{-54}){\rm MeV}\,. \tag{280}$$

A weighted average of the four eligible numbers would yield $[r_0\Lambda_{\overline{\rm MS}}]^{(2)} = 0.709(22)$, not covering the best result and in particular leading to a smaller error than we feel is justified, given the issues discussed previously in Sec. 9.4.2 (Karbstein 14 [9], ETM 11C [71]) and Sec. 9.8.2 (ETM 10F [126]). Thus we believe that our estimate is a conservative choice; the low value of ETM 11C [71] leads to a large downward error. We hope that future work will improve the situation.

For $N_f = 0$ we take into account ALPHA 98 [56], QCDSF/UKQCD 05 [93], and Brambilla 10 [72] for forming a range. We exclude the older estimates shown in the graph which have a limited control of the systematic errors due to power law corrections and discretization errors.[11] None of the computations have a full set of ★ and has P for publication status. Taking a weighted average of the three numbers, we obtain $[r_0\Lambda_{\overline{\rm MS}}]^{(0)} = 0.615(5)$, dominated by the QCDSF/UKQCD 05 [93] result.

Since we are not yet convinced that such a small uncertainty has been reached, we prefer to presently take a range which encompasses all four central values and whose uncertainty comes close to our estimate of the perturbative error in QCDSF/UKQCD 05 [93]: based on $|c_4/c_1| \approx 2$ as before, we find $\Delta[r_0\Lambda_{\overline{\rm MS}}]^{(0)} = 0.018$. We then have

$$[r_0\Lambda_{\overline{\rm MS}}]^{(0)} = 0.62(2)\,. \tag{281}$$

Converting to physical units, again using $r_0 = 0.472\,$fm yields

$$\Lambda^{(0)}_{\overline{\rm MS}} = 260(7)\,{\rm MeV}\,. \tag{282}$$

While the conversion of the Λ parameter to physical units is quite unambiguous for $N_f = 2+1$, our choice of $r_0 = 0.472$ fm also for smaller numbers of flavour amounts to a convention, in particular for $N_f = 0$. Indeed, in the Tabs. 44–49 somewhat different numbers in MeV are found.

How sure are we about our ranges for $[r_0\Lambda_{\overline{\rm MS}}]^{(N_f)}$? In one case we have a result, Eq. (279) which easily passes our criteria, in another one (Eq. (281)) we have three compatible results which are close to that quality and agree. For $N_f = 2+1$ the range (Eq. (277)) takes account of results with rather different systematics. We therefore find it difficult to imagine that the ranges could be violated by much.

[11] We have assigned a ○ for the continuum limit, in Boucaud 00A [131], 00B [130], 01A [129], Soto 01 [128] but these results are from lattices of a very small physical size with finite-size effects that are not easily quantified.

9.9.4 Conclusions

With the present results our range for the strong coupling is (repeating Eq. (276))

$$\alpha_{\overline{\rm MS}}^{(5)}(M_Z) = 0.1182(12) \qquad \text{Refs. [10, 12, 53, 91, 92]},$$

and the associated Λ parameter

$$\Lambda_{\overline{\rm MS}}^{(5)} = 211(14)\ \text{MeV} \qquad \text{Refs. [10, 12, 53, 91, 92]}. \tag{283}$$

These have changed little compared to the previous FLAG review. As can be seen from Fig. 33, when surveying the green data points, the individual lattice results agree within their quoted errors. Furthermore those points are based on different methods for determining α_s, each with its own difficulties and limitations. Thus the overall consistency of the lattice α_s results engenders confidence in our range.

It is interesting to compare to the new Particle Data Group world average, which appeared in February 2016 [4]. The PDG performs their averages, both of lattice determinations and of different categories of phenomenological determinations of α_s, in a way differing significantly from how we determine our range. They perform an unweighted average of the mean values. As its error they use the average of the quoted errors of the different determinations that went into the average. This procedure leads to larger final uncertainties than the one used in the previous edition [5]. When one applies this method to the numbers entering Eq. (276), i.e. the ones satisfying our criteria, one obtains $\alpha_{\overline{\rm MS}}^{(5)}(M_Z) = 0.1181(12)$. This number is close to our result Eq. (276). It differs a little from the value quoted by the PDG since in a couple of cases we used updated results and because not all determinations entering the PDG average satisfy our citeria. For comparison, the PDG number for lattice results is 0.1187(12), and their average of all phenomenological results is 0.1175(17).

Our range for the lattice determination of $\alpha_{\overline{\rm MS}}(M_Z)$ in Eq. (276) is in excellent agreement with the PDG nonlattice average Eq. (232). This is an excellent check for the subtle interplay of theory, phenomenology and experiments in the nonlattice determinations. The work done on the lattice provides an entirely independent determination, with negligible experimental uncertainty, which reaches a better precision even with our conservative estimate of its uncertainty.

We finish by commenting on perspectives for the future. In the next few years we anticipate that a growing number of lattice calculations of α_s from different quantities and by different collaborations will enable increasingly precise determinations, coupled with stringent cross-checks. The determination of α_s from observables at the lattice spacing scale may improve due to a further reduction of the lattice spacing. This reduces $\alpha_{\rm eff}$ and thus the dominating error in $\alpha_{\overline{\rm MS}}$ as long as perturbative results for the simulated action are available to high order. Schrödinger functional methods for $N_f = 2+1$ will certainly reach the precision of the present $N_f = 2$ results soon, as this just requires an application of the presently known techniques. Furthermore, we may expect a significant reduction of errors due to new definitions of running couplings [57, 58] using the Yang Mills gradient flow [13]. Factors of two and more in precision are certainly possible. At this point it will then also be necessary to include the charm quark in the computations such that the perturbative matching of $N_f = 2+1$ and $2+1+1$ theories at the charm quark threshold is avoided. First generation $N_f = 2+1+1$ simulations are presently being carried out.

References

[1] LHC Higgs Cross Section Working Group collaboration, S. Heinemeyer et al., *Handbook of LHC Higgs Cross Sections: 3. Higgs Properties*, 1307.1347.

[2] LBNE collaboration, C. Adams et al., *Scientific Opportunities with the Long-Baseline Neutrino Experiment*, 1307.7335.

[3] S. Dawson, A. Gritsan, H. Logan, J. Qian, C. Tully et al., *Higgs Working Group Report of the Snowmass 2013 Community Planning Study*, 1310.8361.

[4] Particle Data Group collaboration, K. A. Olive et al., *Review of Particle Physics*, *Chin. Phys.* **C38** (2014) 090001 and 2015 update.

[5] Particle Data Group collaboration, J. Beringer et al., *Review of Particle Physics*, *Phys.Rev.* **D86** (2012) 010001 and 2013 partial update for the 2014 edition.

[6] S. Bethke, A. H. Hoang, S. Kluth, J. Schieck, I. W. Stewart et al., *Workshop on Precision Measurements of α_s*, 1110.0016.

[7] W. Bernreuther and W. Wetzel, *Decoupling of heavy quarks in the minimal subtraction scheme*, *Nucl.Phys.* **B197** (1982) 228.

[8] K. Chetyrkin, J. H. Kuhn and C. Sturm, *QCD decoupling at four loops*, *Nucl.Phys.* **B744** (2006) 121–135, [hep-ph/0512060].

[9] [Karbstein 14] F. Karbstein, A. Peters and M. Wagner, $\Lambda_{\overline{\rm MS}}^{(n_f=2)}$ *from a momentum space analysis of the quark-antiquark static potential*, *JHEP* **1409** (2014) 114, [1407.7503].

[10] [Bazavov 14] A. Bazavov, N. Brambilla, X. Garcia i Tormo, P. Petreczky, S. J. and A. Vairo, *Determination of α_s from the QCD static energy: An update*, *Phys.Rev.* **D90** (2014) 074038, [1407.8437].

[11] [FlowQCD 15] M. Asakawa, T. Iritani, M. Kitazawa and H. Suzuki, *Determination of Reference Scales for Wilson Gauge Action from Yang–Mills Gradient Flow*, 1503.06516.

[12] [HPQCD 14A] B. Chakraborty, C. T. H. Davies, G. C. Donald, R. J. Dowdall, B. Galloway, P. Knecht et al., *High-precision quark masses and QCD coupling from $n_f = 4$ lattice QCD*, *Phys.Rev.* **D91** (2015) 054508, [1408.4169].

[13] M. Lüscher, *Properties and uses of the Wilson flow in lattice QCD*, *JHEP* **08** (2010) 071, [1006.4518].

[14] [BMW 12A] S. Borsanyi, S. Dürr, Z. Fodor, C. Hoelbling, S. D. Katz et al., *High-precision scale setting in lattice QCD*, *JHEP* **1209** (2012) 010, [1203.4469].

[15] R. Sommer, *A new way to set the energy scale in lattice gauge theories and its applications to the static force and α_s in SU(2) Yang-Mills theory*, *Nucl. Phys.* **B411** (1994) 839–854, [hep-lat/9310022].

[16] C. W. Bernard et al., *The static quark potential in three flavor QCD*, *Phys. Rev.* **D62** (2000) 034503, [hep-lat/0002028].

[17] G. Martinelli and C. T. Sachrajda, *On the difficulty of computing higher twist corrections*, *Nucl.Phys.* **B478** (1996) 660–686, [hep-ph/9605336].

[18] D. Boito, M. Golterman, K. Maltman, J. Osborne and S. Peris, *Strong coupling from the revised ALEPH data for hadronic τ decays*, *Phys. Rev.* **D91** (2015) 034003, [1410.3528].

[19] L. Del Debbio, H. Panagopoulos and E. Vicari, *Theta dependence of SU(N) gauge theories*, *JHEP* **08** (2002) 044, [hep-th/0204125].

[20] C. Bernard et al., *Topological susceptibility with the improved Asqtad action*, *Phys. Rev.* **D68** (2003) 114501, [hep-lat/0308019].

[21] [ALPHA 10C] S. Schaefer, R. Sommer and F. Virotta, *Critical slowing down and error analysis in lattice QCD simulations*, *Nucl.Phys.* **B845** (2011) 93–119, [1009.5228].

[22] A. Chowdhury, A. Harindranath, J. Maiti and P. Majumdar, *Topological susceptibility in lattice Yang-Mills theory with open boundary condition*, *JHEP* **02** (2014) 045, [1311.6599].

[23] [LSD 14] R. C. Brower et al., *Maximum-Likelihood Approach to Topological Charge Fluctuations in Lattice Gauge Theory*, *Phys. Rev.* **D90** (2014) 014503, [1403.2761].

[24] [HotQCD 14] A. Bazavov et al., *Equation of state in (2+1)-flavor QCD*, *Phys.Rev.* **D90** (2014) 094503, [1407.6387].

[25] [JLQCD 15] H. Fukaya, S. Aoki, G. Cossu, S. Hashimoto, T. Kaneko and J. Noaki, *η' meson mass from topological charge density correlator in QCD*, *Phys. Rev.* **D92** (2015) 111501, [1509.00944].

[26] M. Lüscher and S. Schaefer, *Lattice QCD without topology barriers*, *JHEP* **1107** (2011) 036, [1105.4749].

[27] [ETM 09C] R. Baron et al., *Light meson physics from maximally twisted mass lattice QCD*, *JHEP* **08** (2010) 097, [0911.5061].

[28] [ETM 09] B. Blossier et al., *Pseudoscalar decay constants of kaon and D-mesons from $N_f = 2$ twisted mass lattice QCD*, *JHEP* **0907** (2009) 043, [0904.0954].

[29] [ALPHA 12] P. Fritzsch, F. Knechtli, B. Leder, M. Marinkovic, S. Schaefer et al., *The strange quark mass and the Λ parameter of two flavor QCD*, *Nucl.Phys.* **B865** (2012) 397–429, [1205.5380].

[30] [QCDSF 12] G. Bali, P. Bruns, S. Collins, M. Deka, B. Glasle et al., *Nucleon mass and sigma term from lattice QCD with two light fermion flavors*, *Nucl.Phys.* **B866** (2013) 1–25, [1206.7034].

[31] [HPQCD 09B] C. T. H. Davies, E. Follana, I. Kendall, G. P. Lepage and C. McNeile, *Precise determination of the lattice spacing in full lattice QCD*, *Phys.Rev.* **D81** (2010) 034506, [0910.1229].

[32] [MILC 10] A. Bazavov et al., *Results for light pseudoscalar mesons*, *PoS* **LAT2010** (2010) 074, [1012.0868].

[33] [HotQCD 11] A. Bazavov, T. Bhattacharya, M. Cheng, C. DeTar, H. Ding et al., *The chiral and deconfinement aspects of the QCD transition*, *Phys.Rev.* **D85** (2012) 054503, [1111.1710].

[34] S. Necco and R. Sommer, *The $N_f = 0$ heavy quark potential from short to intermediate distances*, *Nucl.Phys.* **B622** (2002) 328–346, [hep-lat/0108008].

[35] M. Lüscher and P. Weisz, *Quark confinement and the bosonic string*, *JHEP* **0207** (2002) 049, [hep-lat/0207003].

[36] S. Sint and A. Ramos, *On $O(a^2)$ effects in gradient flow observables*, *PoS* **LATTICE2014** (2015) 329, [1411.6706].

[37] Z. Fodor, K. Holland, J. Kuti, S. Mondal, D. Nogradi et al., *The lattice gradient flow at tree-level and its improvement*, *JHEP* **1409** (2014) 018, [1406.0827].

[38] [MILC 15] A. Bazavov et al., *Gradient flow and scale setting on MILC HISQ ensembles*, *Phys. Rev.* **D93** (2016) 094510, [1503.02769].

[39] V. G. Bornyakov et al., *Wilson flow and scale setting from lattice QCD*, 1508.05916.

[40] M. Lüscher, P. Weisz and U. Wolff, *A numerical method to compute the running coupling in asymptotically free theories*, *Nucl.Phys.* **B359** (1991) 221–243.

[41] M. Lüscher, R. Narayanan, P. Weisz and U. Wolff, *The Schrödinger functional: a renormalizable probe for non-abelian gauge theories*, *Nucl. Phys.* **B384** (1992) 168–228, [hep-lat/9207009].

[42] S. Sint, *On the Schrödinger functional in QCD*, *Nucl.Phys.* **B421** (1994) 135–158, [hep-lat/9312079].

[43] A. Coste, A. Gonzalez-Arroyo, J. Jurkiewicz and C. Korthals Altes, *Zero momentum contribution to Wilson loops in periodic boxes*, *Nucl.Phys.* **B262** (1985) 67.

[44] M. Lüscher, R. Sommer, P. Weisz and U. Wolff, *A precise determination of the running coupling in the $SU(3)$ Yang-Mills theory*, *Nucl.Phys.* **B413** (1994) 481–502, [hep-lat/9309005].

[45] S. Sint and R. Sommer, *The running coupling from the QCD Schrödinger functional: a one loop analysis*, *Nucl.Phys.* **B465** (1996) 71–98, [hep-lat/9508012].

[46] [ALPHA 99] A. Bode, P. Weisz and U. Wolff, *Two loop computation of the Schrödinger functional in lattice QCD*, *Nucl.Phys.* **B576** (2000) 517–539, [hep-lat/9911018].

[47] [CP-PACS 04] S. Takeda, S. Aoki, M. Fukugita, K.-I. Ishikawa, N. Ishizuka et al., *A scaling study of the step scaling function in $SU(3)$ gauge theory with improved gauge actions*, *Phys.Rev.* **D70** (2004) 074510, [hep-lat/0408010].

[48] M. Lüscher, *A Semiclassical Formula for the Topological Susceptibility in a Finite Space-time Volume*, *Nucl. Phys.* **B205** (1982) 483.

[49] P. Fritzsch, A. Ramos and F. Stollenwerk, *Critical slowing down and the gradient flow coupling in the Schrdinger functional*, *PoS* **Lattice2013** (2014) 461, [1311.7304].

[50] M. Lüscher, *Step scaling and the Yang-Mills gradient flow*, *JHEP* **06** (2014) 105, [1404.5930].

[51] [ALPHA 10A] F. Tekin, R. Sommer and U. Wolff, *The running coupling of QCD with four flavors*, *Nucl.Phys.* **B840** (2010) 114–128, [1006.0672].

[52] P. Perez-Rubio and S. Sint, *Non-perturbative running of the coupling from four flavour lattice QCD with staggered quarks*, *PoS* **LAT2010** (2010) 236, [1011.6580].

[53] [PACS-CS 09A] S. Aoki et al., *Precise determination of the strong coupling constant in $N_f = 2 + 1$ lattice QCD with the Schrödinger functional scheme*, *JHEP* **0910** (2009) 053, [0906.3906].

[54] [ALPHA 04] M. Della Morte et al., *Computation of the strong coupling in QCD with two dynamical flavours*, *Nucl. Phys.* **B713** (2005) 378–406, [hep-lat/0411025].

[55] [ALPHA 01A] A. Bode et al., *First results on the running coupling in QCD with two massless flavors*, *Phys.Lett.* **B515** (2001) 49–56, [hep-lat/0105003].

[56] [ALPHA 98] S. Capitani, M. Lüscher, R. Sommer and H. Wittig, *Nonperturbative quark mass renormalization in quenched lattice QCD*, *Nucl.Phys.* **B544** (1999) 669–698, [hep-lat/9810063].

[57] Z. Fodor, K. Holland, J. Kuti, D. Nogradi and C. H. Wong, *The Yang-Mills gradient flow in finite volume*, *JHEP* **1211** (2012) 007, [1208.1051].

[58] P. Fritzsch and A. Ramos, *The gradient flow coupling in the Schrödinger functional*, *JHEP* **1310** (2013) 008, [1301.4388].

[59] C. Michael, *The running coupling from lattice gauge theory*, *Phys.Lett.* **B283** (1992) 103–106, [hep-lat/9205010].

[60] [UKQCD 92] S. P. Booth et al., *The running coupling from SU(3) lattice gauge theory*, *Phys. Lett.* **B294** (1992) 385–390, [hep-lat/9209008].

[61] W. Fischler, *Quark-antiquark potential in QCD*, *Nucl.Phys.* **B129** (1977) 157–174.

[62] A. Billoire, *How heavy must be quarks in order to build coulombic $q\bar{q}$ bound states*, *Phys.Lett.* **B92** (1980) 343.

[63] M. Peter, *The static potential in QCD: a full two loop calculation*, *Nucl.Phys.* **B501** (1997) 471–494, [hep-ph/9702245].

[64] Y. Schroder, *The static potential in QCD to two loops*, *Phys.Lett.* **B447** (1999) 321–326, [hep-ph/9812205].

[65] N. Brambilla, A. Pineda, J. Soto and A. Vairo, *The infrared behavior of the static potential in perturbative QCD*, *Phys.Rev.* **D60** (1999) 091502, [hep-ph/9903355].

[66] A. V. Smirnov, V. A. Smirnov and M. Steinhauser, *Three-loop static potential*, *Phys.Rev.Lett.* **104** (2010) 112002, [0911.4742].

[67] C. Anzai, Y. Kiyo and Y. Sumino, *Static QCD potential at three-loop order*, *Phys.Rev.Lett.* **104** (2010) 112003, [0911.4335].

[68] N. Brambilla, A. Vairo, X. Garcia i Tormo and J. Soto, *The QCD static energy at NNNLL*, *Phys.Rev.* **D80** (2009) 034016, [0906.1390].

[69] S. Necco and R. Sommer, *Testing perturbation theory on the $N_f = 0$ static quark potential*, *Phys.Lett.* **B523** (2001) 135–142, [hep-ph/0109093].

[70] A. Bazavov, N. Brambilla, X. Garcia i Tormo, P. Petreczky, J. Soto et al., *Determination of α_s from the QCD static energy*, *Phys.Rev.* **D86** (2012) 114031, [1205.6155].

[71] [ETM 11C] K. Jansen, F. Karbstein, A. Nagy and M. Wagner, $\Lambda_{\overline{\rm MS}}$ *from the static potential for QCD with $N_f = 2$ dynamical quark flavors*, *JHEP* **1201** (2012) 025, [1110.6859].

[72] N. Brambilla, X. Garcia i Tormo, J. Soto and A. Vairo, *Precision determination of $r_0\,\Lambda_{\overline{MS}}$ from the QCD static energy*, *Phys.Rev.Lett.* **105** (2010) 212001, [1006.2066].

[73] G. S. Bali and K. Schilling, *Running coupling and the Λ-parameter from $SU(3)$ lattice simulations*, *Phys.Rev.* **D47** (1993) 661–672, [hep-lat/9208028].

[74] F. Knechtli and B. Leder, *The shape of the static potential with dynamical fermions*, *PoS* **LAT2011** (2011) 315, [1112.1246].

[75] L. R. Surguladze and M. A. Samuel, *Total hadronic cross-section in e+ e- annihilation at the four loop level of perturbative QCD*, *Phys. Rev. Lett.* **66** (1991) 560–563.

[76] S. G. Gorishnii, A. L. Kataev and S. A. Larin, *The $O(\alpha_s^3)$ corrections to $\sigma_{tot}(e^+e^- \to hadrons)$ and $\Gamma(\tau^- \to \nu_\tau + hadrons)$ in QCD*, *Phys. Lett.* **B259** (1991) 144–150.

[77] P. A. Baikov, K. G. Chetyrkin and J. H. Kuhn, *Order α_s^4 QCD Corrections to Z and tau Decays*, *Phys. Rev. Lett.* **101** (2008) 012002, [0801.1821].

[78] I. Balitsky, M. Beneke and V. M. Braun, *Instanton contributions to the τ decay widths*, *Phys.Lett.* **B318** (1993) 371–381, [hep-ph/9309217].

[79] [JLQCD 10] E. Shintani, S. Aoki, H. Fukaya, S. Hashimoto, T. Kaneko et al., *Strong coupling constant from vacuum polarization functions in three-flavor lattice QCD with dynamical overlap fermions*, *Phys.Rev.* **D82** (2010) 074505, Erratum–ibid. **D89** (2014) 099903, [1002.0371].

[80] [JLQCD/TWQCD 08C] E. Shintani et al., *Lattice study of the vacuum polarization function and determination of the strong coupling constant*, *Phys.Rev.* **D79** (2009) 074510, [0807.0556].

[81] R. J. Hudspith, R. Lewis, K. Maltman and E. Shintani, *Determining the QCD coupling from lattice vacuum polarization*, in *Proceedings, 33rd International Symposium on Lattice Field Theory (Lattice 2015)*, vol. LATTICE2015, p. 268, 2016. 1510.04890.

[82] [HPQCD 05A] Q. Mason et al., *Accurate determinations of α_s from realistic lattice QCD*, *Phys. Rev. Lett.* **95** (2005) 052002, [hep-lat/0503005].

[83] [HPQCD 08A] C. T. H. Davies et al., *Update: accurate determinations of α_s from realistic lattice QCD*, *Phys. Rev.* **D78** (2008) 114507, [0807.1687].

[84] G. P. Lepage and P. B. Mackenzie, *On the viability of lattice perturbation theory*, *Phys.Rev.* **D48** (1993) 2250–2264, [hep-lat/9209022].

[85] K. Hornbostel, G. Lepage and C. Morningstar, *Scale setting for α_s beyond leading order*, *Phys.Rev.* **D67** (2003) 034023, [hep-ph/0208224].

[86] A. X. El-Khadra, G. Hockney, A. S. Kronfeld and P. B. Mackenzie, *A determination of the strong coupling constant from the charmonium spectrum*, *Phys.Rev.Lett.* **69** (1992) 729–732.

[87] S. Aoki, M. Fukugita, S. Hashimoto, N. Ishizuka, H. Mino et al., *Manifestation of sea quark effects in the strong coupling constant in lattice QCD*, *Phys.Rev.Lett.* **74** (1995) 22–25, [hep-lat/9407015].

[88] C. T. H. Davies, K. Hornbostel, G. Lepage, A. Lidsey, J. Shigemitsu et al., *A precise determination of α_s from lattice QCD*, *Phys.Lett.* **B345** (1995) 42–48, [hep-ph/9408328].

[89] [SESAM 99] A. Spitz et al., *α_s from upsilon spectroscopy with dynamical Wilson fermions*, *Phys.Rev.* **D60** (1999) 074502, [hep-lat/9906009].

[90] M. Wingate, T. A. DeGrand, S. Collins and U. M. Heller, *From spectroscopy to the strong coupling constant with heavy Wilson quarks*, *Phys.Rev.* **D52** (1995) 307–319, [hep-lat/9501034].

[91] [HPQCD 10] C. McNeile, C. T. H. Davies, E. Follana, K. Hornbostel and G. P. Lepage, *High-precision c and b masses and QCD coupling from current-current correlators in lattice and continuum QCD*, *Phys. Rev.* **D82** (2010) 034512, [1004.4285].

[92] K. Maltman, D. Leinweber, P. Moran and A. Sternbeck, *The realistic lattice determination of $\alpha_s(M_Z)$ revisited*, *Phys. Rev.* **D78** (2008) 114504, [0807.2020].

[93] [QCDSF/UKQCD 05] M. Göckeler, R. Horsley, A. Irving, D. Pleiter, P. Rakow, G. Schierholz et al., *A determination of the Lambda parameter from full lattice QCD*, *Phys.Rev.* **D73** (2006) 014513, [hep-ph/0502212].

[94] [QCDSF/UKQCD 04A] M. Göckeler, R. Horsley, A. Irving, D. Pleiter, P. Rakow, G. Schierholz et al., *Determination of Λ in quenched and full QCD: an update*, *Nucl.Phys.Proc.Suppl.* **140** (2005) 228–230, [hep-lat/0409166].

[95] S. Booth, M. Göckeler, R. Horsley, A. Irving, B. Joo, S. Pickles et al., *The strong coupling constant from lattice QCD with $N_f = 2$ dynamical quarks*, *Nucl.Phys.Proc.Suppl.* **106** (2002) 308–310, [hep-lat/0111006].

[96] [QCDSF/UKQCD 01] S. Booth, M. Göckeler, R. Horsley, A. Irving, B. Joo, S. Pickles et al., *Determination of $\Lambda_{\overline{\rm MS}}$ from quenched and $N_f = 2$ dynamical QCD*, *Phys.Lett.* **B519** (2001) 229–237, [hep-lat/0103023].

[97] [HPQCD 03A] C. T. H. Davies et al., *High-precision lattice QCD confronts experiment*, *Phys. Rev. Lett.* **92** (2004) 022001, [hep-lat/0304004].

[98] Q. J. Mason, *High-precision lattice QCD: Perturbations in a non-perturbative world*. PhD thesis, Cornell U., LNS, 2004.

[99] [HPQCD 08B] I. Allison et al., *High-precision charm-quark mass from current-current correlators in lattice and continuum QCD*, *Phys. Rev.* **D78** (2008) 054513, [0805.2999].

[100] A. Bochkarev and P. de Forcrand, *Determination of the renormalized heavy quark mass in lattice QCD*, *Nucl.Phys.* **B477** (1996) 489–520, [hep-lat/9505025].

[101] K. Chetyrkin, J. H. Kuhn and C. Sturm, *Four-loop moments of the heavy quark vacuum polarization function in perturbative QCD*, *Eur.Phys.J.* **C48** (2006) 107–110, [hep-ph/0604234].

[102] R. Boughezal, M. Czakon and T. Schutzmeier, *Charm and bottom quark masses from perturbative QCD*, *Phys.Rev.* **D74** (2006) 074006, [hep-ph/0605023].

[103] A. Maier, P. Maierhofer and P. Marqaurd, *The second physical moment of the heavy quark vector correlator at $O(\alpha_s^3)$*, *Phys.Lett.* **B669** (2008) 88–91, [0806.3405].

[104] A. Maier, P. Maierhofer, P. Marquard and A. Smirnov, *Low energy moments of heavy quark current correlators at four loops*, *Nucl.Phys.* **B824** (2010) 1–18, [0907.2117].

[105] Y. Kiyo, A. Maier, P. Maierhofer and P. Marquard, *Reconstruction of heavy quark current correlators at $O(\alpha_s^3)$*, *Nucl.Phys.* **B823** (2009) 269–287, [0907.2120].

[106] J. H. Kühn, M. Steinhauser and C. Sturm, *Heavy quark masses from sum rules in four-loop approximation*, *Nucl. Phys.* **B778** (2007) 192–215, [hep-ph/0702103].

[107] K. Chetyrkin, J. Kuhn, A. Maier, P. Maierhofer, P. Marquard et al., *Charm and Bottom Quark Masses: An Update*, *Phys.Rev.* **D80** (2009) 074010, [0907.2110].

[108] [HPQCD 10B] H. Na, C. T. H. Davies, E. Follana, G. P. Lepage and J. Shigemitsu, *The $D \to K\ell\nu$ semileptonic decay scalar form factor and $|V_{cs}|$ from lattice QCD*, *Phys.Rev.* **D82** (2010) 114506, [1008.4562].

[109] [HPQCD 12F] R.J. Dowdall, C. Davies, T. Hammant and R. Horgan, *Precise heavy-light meson masses and hyperfine splittings from lattice QCD including charm quarks in the sea*, *Phys. Rev.* **D86** (2012) 094510, [1207.5149].

[110] [HPQCD 13A] R. Dowdall, C. Davies, G. Lepage and C. McNeile, *V_{us} from π and K decay constants in full lattice QCD with physical u, d, s and c quarks*, *Phys.Rev.* **D88** (2013) 074504, [1303.1670].

[111] [JLQCD 15B] K. Nakayama, B. Fahy and S. Hashimoto, *Charmonium current-current correlators with Mobius domain-wall fermion*, in *Proceedings, 33rd International Symposium on Lattice Field Theory (Lattice 2015)*, vol. LATTICE2015, p. 267, 2016. 1511.09163.

[112] A. Cucchieri, *Gribov copies in the minimal Landau gauge: The Influence on gluon and ghost propagators*, *Nucl.Phys.* **B508** (1997) 353–370, [hep-lat/9705005].

[113] L. Giusti, M. Paciello, C. Parrinello, S. Petrarca and B. Taglienti, *Problems on lattice gauge fixing*, *Int.J.Mod.Phys.* **A16** (2001) 3487–3534, [hep-lat/0104012].

[114] A. Maas, J. M. Pawlowski, D. Spielmann, A. Sternbeck and L. von Smekal, *Strong-coupling study of the Gribov ambiguity in lattice Landau gauge*, *Eur.Phys.J.* **C68** (2010) 183–195, [0912.4203].

[115] B. Alles, D. Henty, H. Panagopoulos, C. Parrinello, C. Pittori et al., *α_s from the nonperturbatively renormalised lattice three gluon vertex*, *Nucl.Phys.* **B502** (1997) 325–342, [hep-lat/9605033].

[116] [Boucaud 01B] P. Boucaud, J. Leroy, H. Moutarde, J. Micheli, O. Pene et al., *Preliminary calculation of α_s from Green functions with dynamical quarks*, *JHEP* **0201** (2002) 046, [hep-ph/0107278].

[117] P. Boucaud, J. Leroy, A. Le Yaouanc, A. Lokhov, J. Micheli et al., *Asymptotic behavior of the ghost propagator in SU(3) lattice gauge theory*, *Phys.Rev.* **D72** (2005) 114503, [hep-lat/0506031].

[118] P. Boucaud, J. Leroy, A. Le Yaouanc, A. Lokhov, J. Micheli et al., *Non-perturbative power corrections to ghost and gluon propagators*, *JHEP* **0601** (2006) 037, [hep-lat/0507005].

[119] A. Sternbeck, K. Maltman, L. von Smekal, A. Williams, E. Ilgenfritz et al., *Running α_s from Landau-gauge gluon and ghost correlations*, *PoS* **LAT2007** (2007) 256, [0710.2965].

[120] Ph. Boucaud, F. De Soto, J. Leroy, A. Le Yaouanc, J. Micheli et al., *Ghost-gluon running coupling, power corrections and the determination of $\Lambda_{\overline{\rm MS}}$*, *Phys.Rev.* **D79** (2009) 014508, [0811.2059].

[121] [ETM 13D] B. Blossier et al., *High statistics determination of the strong coupling constant in Taylor scheme and its OPE Wilson coefficient from lattice QCD with a dynamical charm*, *Phys.Rev.* **D89** (2014) 014507, [1310.3763].

[122] [ETM 12C] B. Blossier, P. Boucaud, M. Brinet, F. De Soto, X. Du et al., *The strong running coupling at τ and Z_0 mass scales from lattice QCD*, *Phys.Rev.Lett.* **108** (2012) 262002, [1201.5770].

[123] [ETM 11D] B. Blossier, P. Boucaud, M. Brinet, F. De Soto, X. Du et al., *Ghost-gluon coupling, power corrections and $\Lambda_{\overline{\rm MS}}$ from lattice QCD with a dynamical charm*, *Phys.Rev.* **D85** (2012) 034503, [1110.5829].

[124] A. Sternbeck, K. Maltman, M. Müller-Preussker and L. von Smekal, *Determination of $\Lambda_{\overline{\rm MS}}$ from the gluon and ghost propagators in Landau gauge*, *PoS* **LAT2012** (2012) 243, [1212.2039].

[125] A. Sternbeck, E.-M. Ilgenfritz, K. Maltman, M. Müller-Preussker, L. von Smekal et al., *QCD Lambda parameter from Landau-gauge gluon and ghost correlations*, *PoS* **LAT2009** (2009) 210, [1003.1585].

[126] [ETM 10F] B. Blossier et al., *Ghost-gluon coupling, power corrections and $\Lambda_{\overline{\rm MS}}$ from twisted-mass lattice QCD at $N_f = 2$*, *Phys.Rev.* **D82** (2010) 034510, [1005.5290].

[127] E.-M. Ilgenfritz, C. Menz, M. Müller-Preussker, A. Schiller and A. Sternbeck, *$SU(3)$ Landau gauge gluon and ghost propagators using the logarithmic lattice gluon field definition*, *Phys.Rev.* **D83** (2011) 054506, [1010.5120].

[128] F. De Soto and J. Rodriguez-Quintero, *Notes on the determination of the Landau gauge OPE for the asymmetric three gluon vertex*, *Phys.Rev.* **D64** (2001) 114003, [hep-ph/0105063].

[129] [Boucaud 01A] P. Boucaud, A. Le Yaouanc, J. Leroy, J. Micheli, O. Pene et al., *Testing Landau gauge OPE on the lattice with a $\langle A^2 \rangle$ condensate*, *Phys.Rev.* **D63** (2001) 114003, [hep-ph/0101302].

[130] [Boucaud 00B] P. Boucaud, A. Le Yaouanc, J. Leroy, J. Micheli, O. Pene et al., *Consistent OPE description of gluon two point and three point Green function?*, *Phys.Lett.* **B493** (2000) 315–324, [hep-ph/0008043].

[131] [Boucaud 00A] P. Boucaud, G. Burgio, F. Di Renzo, J. Leroy, J. Micheli et al., *Lattice calculation of $1/p^2$ corrections to α_s and of $\Lambda_{\rm QCD}$ in the MOM scheme*, *JHEP* **0004** (2000) 006, [hep-ph/0003020].

[132] [Becirevic 99B] D. Bećirević, P. Boucaud, J. Leroy, J. Micheli, O. Pene et al., *Asymptotic scaling of the gluon propagator on the lattice*, *Phys.Rev.* **D61** (2000) 114508, [hep-ph/9910204].

[133] [Becirevic 99A] D. Bećirević, P. Boucaud, J. Leroy, J. Micheli, O. Pene et al., *Asymptotic behavior of the gluon propagator from lattice QCD*, *Phys.Rev.* **D60** (1999) 094509, [hep-ph/9903364].

[134] [Boucaud 98B] P. Boucaud, J. Leroy, J. Micheli, O. Pene and C. Roiesnel, *Three loop beta function and nonperturbative α_s in asymmetric momentum scheme*, *JHEP* **9812** (1998) 004, [hep-ph/9810437].

[135] [Boucaud 98A] P. Boucaud, J. Leroy, J. Micheli, O. Pene and C. Roiesnel, *Lattice calculation of α_s in momentum scheme*, *JHEP* **9810** (1998) 017, [hep-ph/9810322].

[136] [ETM 13] K. Cichy, E. Garcia-Ramos and K. Jansen, *Chiral condensate from the twisted mass Dirac operator spectrum*, *JHEP* **1310** (2013) 175, [1303.1954].

[137] [ALPHA 14A] M. Bruno, J. Finkenrath, F. Knechtli, B. Leder and R. Sommer, *Effects of Heavy Sea Quarks at Low Energies*, *Phys. Rev. Lett.* **114** (2015) 102001, [1410.8374].